SURFACE VIBRATORY COMPACTION OF A GRANULAR MATERIAL

A THESIS

Presented to

The Faculty of the Division of Graduate Studies and Research

By

Joe Frank Skelton

In Partial Fulfillment

of the Requirements for the Degree

Doctor of Philosophy in the

School of Civil Engineering

Georgia Institute of Technology

June, 1973

SURFACE VIBRATORY COMPACTION

OF A GRANULAR MATERIAL

Approved:

Dr. W. F. Brumund, Chairman

Professor George F. Sowers

Dr. B. B. Mazanti

Date approved by Chairman: 5/21/73

ACKNOWLEDGMENTS

Throughout this research many hours of critical guidance and consultation were provided by Dr. William F. Brumund. The author wishes to give his genuine thanks to Dr. Brumund for this valuable aid.

Special gratitude is expressed to Dr. B. B. Mazanti and Regents Professor G. F. Sowers for their guidance and comments in the preparation of this work.

The author wishes to express his sincere appreciation to R. L. Brown and R. Joyner for their aid in the construction and instrumentation required in this research.

Special thanks is given to Duke Power Company for the financial assistance given to this research.

Finally, the author wishes to acknowledge the continual encouragement given by his wife, Deanna, and the typing of this work by her.

TABLE OF CONTENTS

Page

LIST OF TABLES

Table Page

LIST OF FIGURES

Figure Page

Figure Page

NOMENCLATURE

A_p	peak-to-peak amplitude of vibration
B	vibrating plate diameter
c	damping constant
c_c	critical damping constant
D	c/c_c = damping ratio
D_R	relative density
e	void ratio
E_{TR}	steady-state transmitted energy per cycle of loading
F_{avg}	average downward force
F_d	dynamic force
F_o	magnitude of impressed force
F_{TR}	force transmitted to base in one dimensional lumped parameter model
F_{max}	maximum downward force
F_{min}	minimum downward force
H_o	original height of confined sample
k	spring constant
L	distance between soil strain gages
M	mass of vibrating plate
q	static bearing capacity of a plate
S_{60}	settlement after 60 minutes
t	time

V_v	volume of voids
W	static force
X	magnitude of the steady-state oscillation
θ	phase angle between transmitted force and displacement
ϕ	phase angle between the vibrational movement and the impressed force
ϕ'	friction angle of sand
γ	unit weight of sand
ψ	phase angle between impressed force and transmitted force
ω	angular velocity
ω_N	undamped natural angular velocity
σ_1	axial stress
σ_3	confining stress

SUMMARY

A review of past research efforts indicated that of the many factors which have been proposed as governing the settlement of vibratory compactors, two factors, acceleration and steady-state transmitted energy per load cycle, have been advanced in recent years as the major factors. However, one recent study has indicated that steady-state transmitted energy and not acceleration is the major factor governing settlement of a vibratory compactor.

In order to examine the concept of steady-state transmitted energy per load cycle as a governing factor in settlements produced by vibratory compactors, settlements of a circular plate vibrating on the surface of a sand mass and on the surface of a small confined sand sample were studied. The relative density of the sand could be varied as well as the static force, dynamic force, and frequency of vibration acting on the circular plate, and the resulting amplitude of plate vibration, plate contact force, and plate settlement could be measured. Movements within the sand mass due to the surface vibrational loading were also able to be measured using electrical inductance soil strain gages.

This study produced several results. First, there

was a linear relationship between settlement of a circular footing and the steady-state transmitted energy per cycle of load application. This linear relationship was found to be a function of the relative density of the sand mass, as well as a function of the type of sand.

Second, for approximately equal steady-state transmitted energy levels, different frequencies of plate vibration were found to cause approximately equal movements within the sand mass, and, therefore, no dependence on frequency was noted.

Finally, densification of the small confined sand samples was observed to be a linear function of the logarithm of the steady-state transmitted energy. A direct correlation between the densification of the confined samples and any densification which occurred in the unconfined samples was not possible due to the different confining conditions. The general shape of the densification-logarithm of steady-state transmitted energy curves were thought to be the same for both the confined and unconfined samples.

CHAPTER I

INTRODUCTION

Factors influencing the vibratory compaction of granular materials have been the object of many studies. Some authorities have tried to show that acceleration is the governing factor controlling the compaction of granular material. Other researchers have sought to show that cyclic shear strain is the governing factor. Still other studies have been made claiming that static weight, amplitude of vibration, and many other variables were the governing factors. None of these research efforts, however, have provided a method for using that particular governing factor as a method for predicting the amount of compaction a given compactor acting on a granular material will produce.

A theory stating that the energy transmitted by a compactor to the granular material is related to the settlement of the compactor has been proposed by Brumund (4)*. This concept seems to provide a consistent viable means of explaining the compaction process. However, no direct correlation has yet been developed between surface

---

*Numbers in parentheses refer to references in Bibliography.

settlement and densification.

The object of this present study was to further expand this transmitted energy concept as well as to observe the overall response of a sand mass subjected to a vibratory surface load.

CHAPTER II

LITERATURE REVIEW

Past study of soil response to vibrations has been divided into three general categories. These categories were analytical models, laboratory experiments, and field studies.

Analytical Models

Reissner (32) developed one of the first analytical solutions for a vibration of a circular vibrator exerting an uniform cyclic pressure at the surface of a material. This material was assumed to be a homogeneous, isotropic, semi-infinite elastic half-space. Sung (39) and Quinlin (31) both expanded Reissner's solution to encompass other pressure distributions developed by long rectangular areas and circular areas. Lysmer (23) and Lysmer and Richart (24) developed the connection between the theory of the elastic-half-space and the mass-spring-dashpot (lumped parameter) system. Richart (33), Richart and Whitman (34), and Whitman and Richart (48) presented the application of the lumped parameter system to the analysis and design of foundations subjected to vibrations. The general purpose

of these theories and models was mainly concerned with describing the steady-state response of the soil-vibrator system and not with changes in the soil such as evidenced by the residual settlements of the vibrator.

Laboratory Experiments

Most experimental work has been conducted utilizing three general methods of applying vibratory loads to a granular material. These were applying loads through a vibrating plate to the surface of (i) a confined sample (the entire surface of the sample loaded with lateral support provided by molds), (ii) an unconfined sample (loaded surface area is small in comparison to the entire surface area of the sample and the depth is many times the loaded area) and (iii) applying loads using a vibrating base support of the sample.

Confined Sample Loading

Barkan (1) stated that experimental work indicated that the inertial force, as determined from acceleration, was the principal vibration parameter. He concluded that since there were very little differences in the specific gravities of granular soils that acceleration was the key parameter governing compaction due to vibrations. He further proposed the presence of a threshold acceleration above which compaction due to vibration occurred. This "threshold of compaction", as Barkan called it, depends on

the void ratio of the granular material and on the static normal stresses. In his paper to the New Mexico Symposium, Barkan (2) referred to a "threshold velocity" rather than the threshold acceleration as being the parameter determining settlement due to vibrations.

Tschebotarioff and McAlpin (44) determined from their research that axial deformation was not dependent on the frequency of vibration but was a function of the number of loading cycles applied to the samples. Their results applied to non-resonant frequency applications only.

Timmerman and Wu (42) conducted confined sample tests using mainly Ottawa sand. They performed these tests keeping accelerations much lower than 0.5 g (g is the acceleration of gravity) in order to determine a relationship between stress and deformation. They also used vibration frequencies of between 2.5 Hz. and 25 Hz. Timmerman and Wu concluded that for accelerations of 0.1 g or less the shear deformations are the principal portion of the soil deformation due to cyclic loading.

Unconfined Sample Loading

The first extensive experimental work in foundation response to vibrations was conducted in Germany by Deutschen Forschungsgesellschaft für Bodenmeckanik (DEGEBO) between 1928 and 1936. From this work, Hertwig, Früh, and Lorenz (16) presented an extensive analysis of the response

of a plate, resting on a soil mass, due to vertical vibrations of the plate. They tried to describe the response by using a single-degree-of-freedom mass-spring-dashpot system. However, this model would only work when some mass of the soil directly under the plate vibrated together as a single mass with the plate. The size of this soil mass depended on many different variables such as frequency, size of plate, dynamic force magnitude, and others. Thus, this added soil mass was required to allow the predicted response to conform with the observed, and, therefore, this predictive method was not realistic since no soil actually vibrated as part of the loading plate.

Eastwood (12) studied the frequency response of a soil-vibrator system subjected to a wide range of loadings. The sand mass used in this study was 4' x 4' x 4' in size with the loading plates being six to ten inches in diameter. He concluded that the resonant frequency of the system decreased if either the size of the vibrating footing (static stress held constant) or the static pressure (size of footing held constant) was increased.

Robson (35), after comparing his experimental results with a lumped-parameter system, concluded that the soil reacted to vibrations as a non-linear spring. His tests indicated that increasing the magnitude of the dynamic force decreased the resonant frequency.

Tanimoto (40) examined the effects of frequency of vibration, length of time of vibration, static weight of a vibrator and acceleration on sand samples. A 10 cm diameter vibrator was used to load a sample 50 cm x 50 cm x 15 cm. The conclusions were that increasing the weight of the vibrator increased the amount of volume change and that density after vibrating was a function of the logarithm of acceleration.

Taylor, Green and Kalita (41) in studying the frequency response of five to nine inch diameter plates vibrating on the surface of a sample found much the same response to static contact pressure as that which Eastwood determined. This study also concluded that as the dynamic stress increased the resonant frequency decreased.

Elastic half-space analysis was compared with constant pressures, amplitudes of vibration, and frequency of vibration obtained from tests of a six inch diameter plate vibrating on the surface of a sand sample 54 inches square and 49 inches deep by Ho and Burwash (17). This study presented data concerning the phase angle between displacement and impressed dynamic force for various frequencies of load application.

Chae (6) performed an experimental investigation of the dynamic behavior of an embedded foundation-soil system using small-scale model tests. From this investigation,

Chae concluded that the amplitude of vibration of an embedded foundation was greatly reduced over the amplitude of a non-embedded foundation. However, the resonant frequency of the system was found to be unaffected by embedment.

Brumund (4) and Brumund and Leonards (5) after much experimental research concluded that steady-state transmitted energy per cycle of load application of a vibratory surface load was the parameter that governed the ultimate settlement of a footing vibrating on a granular soil. Brumund showed, using a sand sample 2' x 2' x 2' and a four inch diameter footing, that settlement of a footing was a linear function of steady-state transmitted energy. This research indicated that the transmitted energy concept was valid for a wide range of frequencies, static weights and dynamic forces. Acceleration was shown not to be the sole factor governing footing settlement as so many researchers had sought to prove. The results of this research were determined from tests using a four inch diameter foot vibrating on an eight cubic foot sample of granular material. The sand was an uniformly graded Ottawa sand placed at a 70% relative density for each test. This study opened a whole new approach to the vibration-settlement problem.

Vibrating Base Support

Using a sand tank 2.2 cm x 17.5 cm x 6.0 cm in size, Mogami and Kubo (25) experimentally concluded that there was little or no densification for accelerations below 1 g. However, they indicated that increasing the acceleration above 1 g caused the densification to increase as the acceleration increased. At an acceleration between 2.5 g and 4 g the maximum density of the material was obtained and any further increase in acceleration caused a decrease in density due to "overvibration" of the material.

Forssblad (13), using small cylindrical samples compacted on a vibrating table, found that the density of the samples increased with acceleration. The density increase was practically linear through the 2 to 3 g acceleration level, while above this acceleration level the rate of density increase was much lower.

Prakash and Gupta (30) studied the vibratory compaction of sand using a 30 cm x 30 cm x 15 cm sample and concluded that acceleration dictates the amount of density increase that a sand will have upon vibration. This conclusion held true for accelerations up to 1.1 g. Above this acceleration there was noted a decrease (overvibration phenomenon) in density. This study also found that a steady-state condition of no density increase occurred after four to ten minutes of vibration. The sample size

used in this study was 30 cm x 30 cm x 15 cm.

Using four different Ottawa sands, a vibrating table, and samples contained in steel molds which were five inches in diameter and 5.5 inches high, Greenfield and Misiaszek (15), after analyzing the test results, found that the parameter controlling densification was acceleration.

A study by D'Appolonia and D'Appolonia (8) produced agreement with previous researchers that up to 1.0 g acceleration there was little densification. This conclusion was reached from separate tests on sand and steel balls. Maximum density was reached for accelerations in the vicinity of 2.0 g.

D'Appolonia (10, 11) arrived at approximately the same conclusion as did Ortigosa (29) and others concerning the cause of the small amount of densification below 1.0 g acceleration. Repeated stress applications and inertia effects appeared to be the most critical parameters. Tests indicated that for frequencies of 10 Hz. or below the amount of nonrecoverable vertical strain was unaffected by frequency. The nonrecoverable vertical strain was found to be a linear function of the logarithm of the loading cycles (up to 6×10^6 cycles).

Ortigosa (29) and Whitman and Ortigosa (47) concluded that for accelerations below 1.0 g there is essentially no densification even with low confining stresses.

Densification below 1.0 g acceleration is due to dynamic stresses only. A further conclusion was that densification could be accomplished with pure dynamic stresses or pure accelerations. These studies also determined that there is a minimum acceleration which is a function of confining stress and initial density required to begin densification. These conclusions were reached after tests performed on Ottawa sand placed in a four inch diameter oedometer, confined, and vibrated on a vibrating table.

Youd (49), using a direct shear device attached to a shaker table, studied the effects of horizontal vibrations on a confined sample of Ottawa sand. Youd proposed that shear distortion activates both densification and dilitation of the material. At low strains, densification predominates while at high strains dilitation dominates. He concluded from his experiments that the void ratio decreases exponentially with acceleration. He also agreed with Barkan's no densification until some threshold acceleration is surpassed.

Using simple shear equipment the Norwegian Geotechnical Institutes developed, Silver and Seed (37) subjected silica sand samples to cyclic strain applications. Their experiments indicated that in determining volume change a fundamental parameter may be the cyclic shear strain.

Field Studies

Converse (7), using a small size test area, studied the compaction of sand by surface vibration. Frequency variations were observed as well as the determination of resonant frequencies for various sizes and weights of vibrator. The results of these experiments also indicated that the maximum density of the sand after vibration was located some depth below the surface of the sand.

Without studying the effects of dynamic force variations Johnson and Sallberg (18) compared the compaction produced by static and vibratory field compactors. From these comparative tests, the heaviest compactors produced the better compaction results.

Lewis (21, 22) investigated the compaction of several different types of soils. These investigations indicated that as the static weight of a field compactor increased the amount of compaction or density change of the sand also increased. High amplitude (one to two inches) plate compactors were the only exceptions to this result. This result agreed with that proposed by Johnson and Sallberg.

Fry (14) conducted research on the effects of vibration on various size foundation footings. Subjecting these footings to various loadings, Fry reported the frequency response of the footings as well as some pressure and settlement data.

Forssblad (13), in addition to his laboratory research, performed field compaction tests using different types of compactors. His tests yielded results which agreed with other researchers. He found, as did Converse, that the maximum density after vibration occurred at some depth within the soil mass. The effect of static pressure was observed to agree with the results reported by Johnson, Sallberg and Lewis. Forssblad did indicate that the higher the dynamic stress was the better the compaction. He also proposed that frequency of vibration should be at or above resonance to optimize compaction.

Moorhouse and Baker (27) conducted tests using a vibrating roller compactor. These tests on saturated sand produced density data as a function of the number of vibrator passes. Density data as a function of depth was also obtained.

D'Appolonia, Whitman and D'Appolonia (9), using two different sizes of compactor, conducted field tests. The major parameters controlling the compaction produced by the vibrating rollers were indicated to be the maximum and minimum dynamic stresses in the soil.

Novak (28) and Moore (26) compared observed vibration amplitudes at resonance to those predicted by mathmatical models. Novak used the model based on a rigid body vibrating on an elastic half-space. From this comparison, Novak

proposed that the mathmatical model could be used to predict resonant frequency and amplitude if some correction factor from field tests was applied. Moore used Sung's model for comparison. He concluded that for small footings on sandy silty soils, the size of the mass ratio causes the pressure distribution to change from parabolic to rigid as the mass ratio increases.

CHAPTER III

HYPOTHESIS

A review of the literature has shown that several factors have been proposed as governing the settlement of vibratory compactors. Two different factors, acceleration and steady-state transmitted energy per load cycle in recent years have been advanced as the major influence in the settlement of vibratory compactors. However, a recent study has indicated that for constant steady-state transmitted energy the settlement of a vibrator is constant over a wide range of accelerations. Thus there is some evidence to indicate that steady-state transmitted energy may be the factor governing the settlement of a vibrator.

To examine the concept that steady-state transmitted energy per load cycle is the major factor governing settlement, the relationship between steady-state transmitted energy and settlement for various frequencies of vibration, static loads, dynamic loads, and initial relative densities of a granular soil was needed. It was thought that for any initial relative density settlement was probably a linear function of the steady-state transmitted energy for any combination of frequency, static load, and dynamic load. As the initial relative density of the granular material

increased, the slope of the linear settlement-steady-state transmitted energy relation should decrease.

The settlement of a vibrator is due to shear distortion and densification of the granular material. The beneficial effects of vibrating a material are achieved due to the increase in the density (densification) of the material. Therefore, a relation between densification and steady-state transmitted energy is essential. It was thought that densification was possibly a linear function of the logarithm of the steady-state transmitted energy.

Finally, many researchers have suggested that the optimum benefits from a vibrator are attained when the vibrator operates at or above the resonant frequency of vibrator-soil system. To substantiate this hypothesis required further research and more data as to what movements are occurring within a granular soil mass subjected to surface vibrational loading.

CHAPTER IV

IDEALIZED VIBRATING SYSTEM

A lumped-parameter one degree of freedom vibrating system was assumed for this laboratory study. A model based on this assumption is shown in Figure 1. Using this model, the governing differential equation, Thomson (43), is

$$M\left(\frac{d^2x}{dt^2}\right) + c\left(\frac{dx}{dt}\right) + kx = F_o \sin\omega t \qquad (1)$$

Where:

M = mass of vibrating plate

c = damping constant (dash pot)

k = spring constant

x = displacement of plate

F_o = magnitude of impressed force

t = time

ω = angular velocity

Equation's 1 solution is

$$x = X_1 e^{-D\omega_n t} \sin\left(\sqrt{1 - D^2}\,\omega_n t + \phi_1\right) + X\sin(\omega t - \phi) \qquad (2)$$

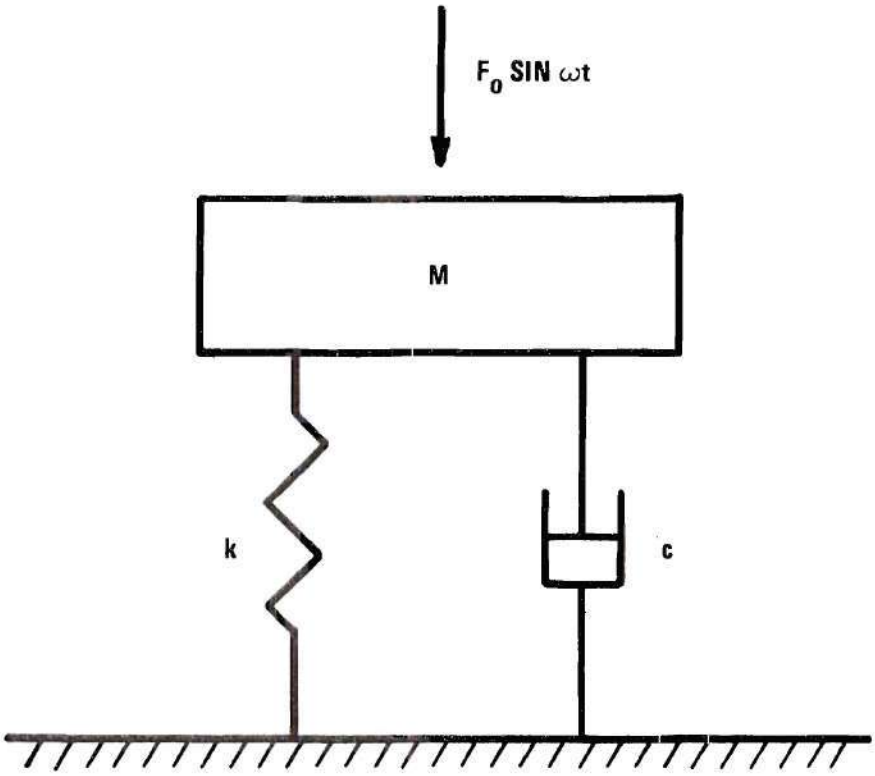

Figure 1. Lumped Parameter Model

Where:

$D = c/c_c$

$c_c = 2M\omega_n$

$\omega_n = \sqrt{k/M}$ = undamped natural frequency

However for steady-state vibrational conditions, the initial term of this equation approaches zero and Equation 2 becomes

$$x = X\sin(\omega t - \phi) \tag{3}$$

Where:

X = magnitude of the steady-state oscillation

ϕ = phase angle between the vibrational movement and the impressed force

Using this solution in Equation 1 gives

$$M\omega^2 X\sin(\omega t - \phi) - c\omega X\sin(\omega t - \phi + \pi/2) - kX\sin(\omega t - \phi) + F_o\sin\omega t = 0 \tag{4}$$

Figure 2 reveals a vectorial representation of Equation 4.

From Figure 2, the force transmitted by the vibrating plate is equal to the force of the spring plus the force of the dash pot. The magnitude of this transmitted force is

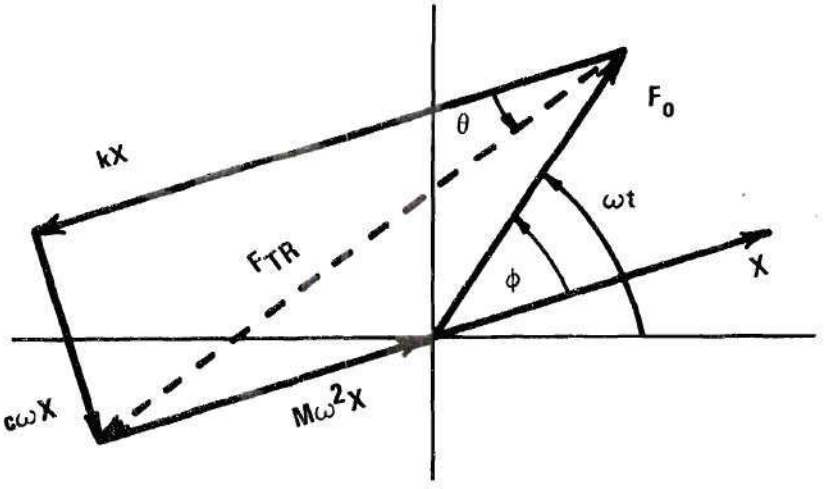

Figure 2. Vectorial Representation of Model Response

$$F_{TR} = \sqrt{(kX)^2 + (c\omega X)^2} \qquad (5)$$

The steady-state response of a vibrating plate is shown in Figure 3. The transmitted energy is equal to the area under the contact force versus vibratory displacement curve, shown as the shaded area in Figure 3. If the vibrating system has small damping, the transmitted energy may be determined using Equation 6.

$$E_{TR} = F_{TR} \cdot A_p \qquad (6)$$

Where:

$$F_{TR} = \frac{F_{max} - F_{min}}{2} \qquad (7)$$

F_{max} = maximum downward force

F_{min} = minimum downward force

A_p = peak-to-peak amplitude

This equation is valid only when there is little or no phase shift between the contact force and vibratory displacement and when the wave is sinusoidal. These conditions then result in a linear relation between F_{max} and F_{min}, and therefore Equation 6 is valid. The values of F_{max} and F_{min} were obtained from a load cell output, while the value of A_p was measured from the output of a LVDT.

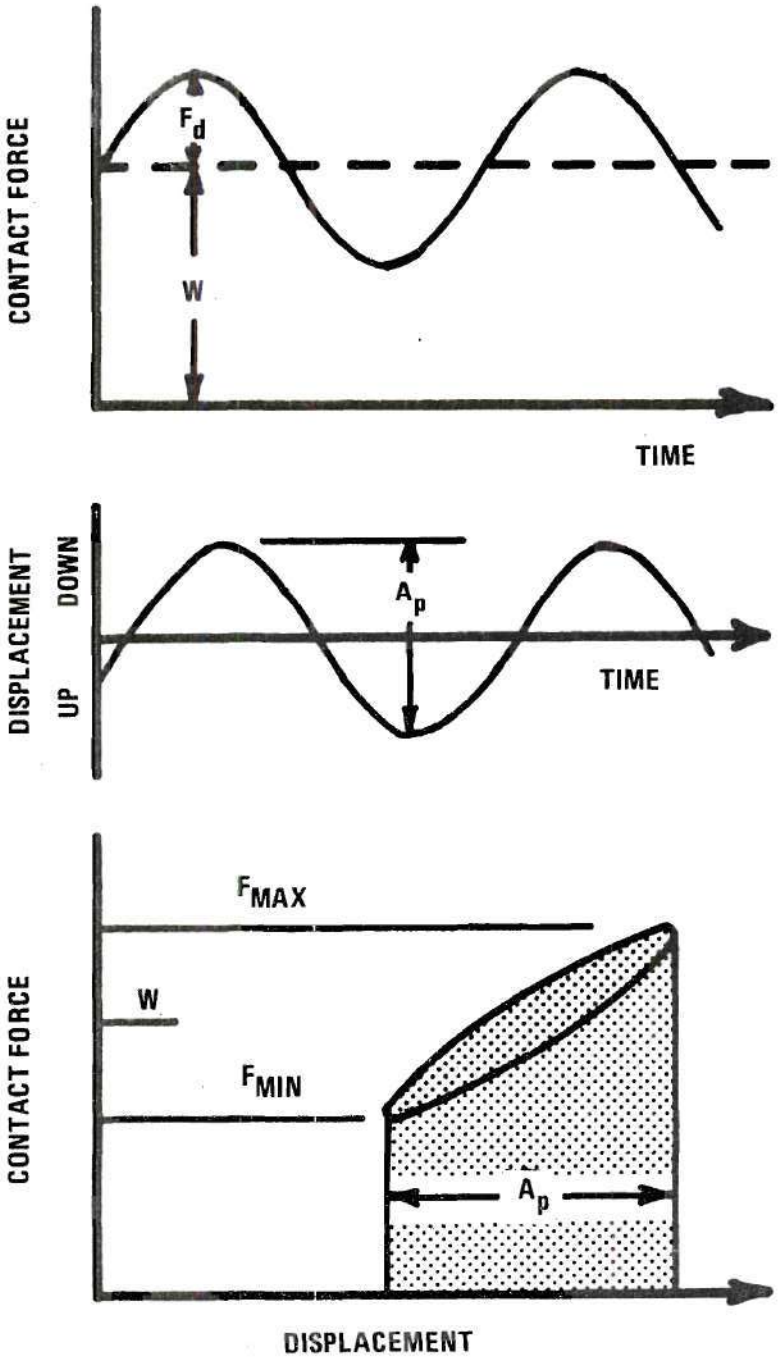

Figure 3. Idealized Response of Vibrating Plate

CHAPTER V

EQUIPMENT

Sand

The only material used for testing in this project was a Rollo washed Georgia sand. The material was composed mainly of quartz, calcium carbonate, and mica particles. All these particles tended to be angular in shape. The average sphericity was 0.9 while the average roundness was 0.5, Krumbein and Sloss (20). The mica represented approximately less than 0.01% by weight of the material.

The general properties of this material were determined. The specific gravity was found to be 2.63. The grain size distribution curve for this material is shown in Figure 4. From this figure, the uniformity coefficient for this material was calculated to be 2.53. Tests were performed on the material and from these tests the maximum and minimum unit weights were determined. The maximum unit weight was found to be 105.2 lbs/ft^3 (minimum void ratio of 0.56) while the minimum unit weight was determined to be 86.9 lbs/ft^3 (maximum void ratio of 0.89). The data for all these tests and the results of triaxial shear tests are given in Appendix A.

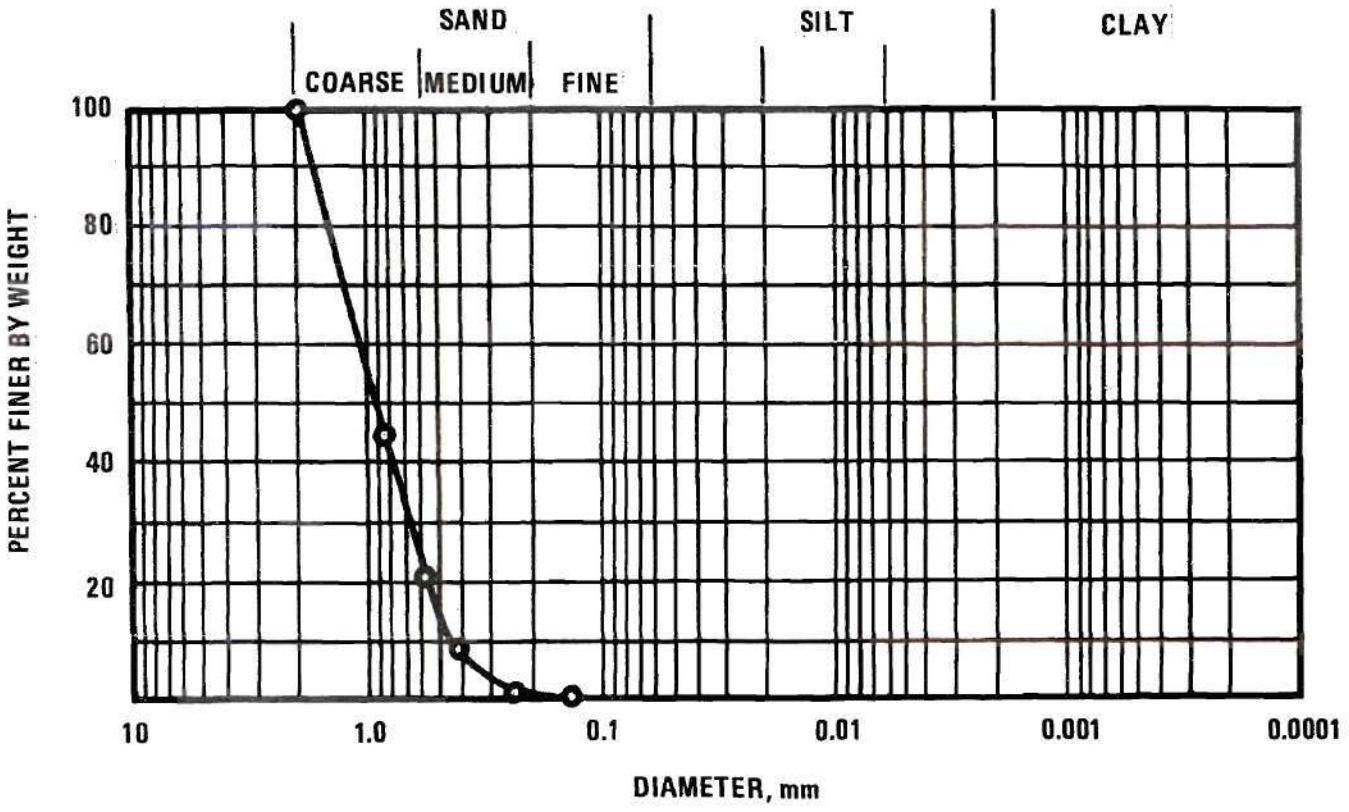

Figure 4. Sand Grain Size Distribution

Sand Placement Apparatus

A "raining" method of sand placement was adopted, Kolbuszewski (19), Walker and Whitaker (46). The sand raining was accomplished using an aluminum box 45" x 45" x 30" with holes drilled in the bottom. By providing two bottom plates with predrilled holes and allowing one to move relative to the other, the raining process could be stopped and started at will. The pattern of holes in the bottom is shown in Figure 5; at the corners additional holes were drilled because of the increased wall friction on the sand near the corners. The increased friction on the sand caused the sand to flow out of the box more slowly unless there was a larger hole area in the corners. The movable lower plate was moved to different positions by means of a lever system. The lever could be moved so as to cause the holes of one plate to align with those of the other plate totally, partially, or not at all. Thus the amount of sand flowing out of the apparatus was able to be varied and controlled. The box and lever system are shown in Figure 6. Below the movable plate, there was a piece of 1/4 inch hardware cloth. This cloth, located approximately six inches below the movable plate, acted as a diffusing screen. The sand fell from the box and struck the cloth. After striking this cloth, the fall of the sand became more scattered and more closely approximated a true raining

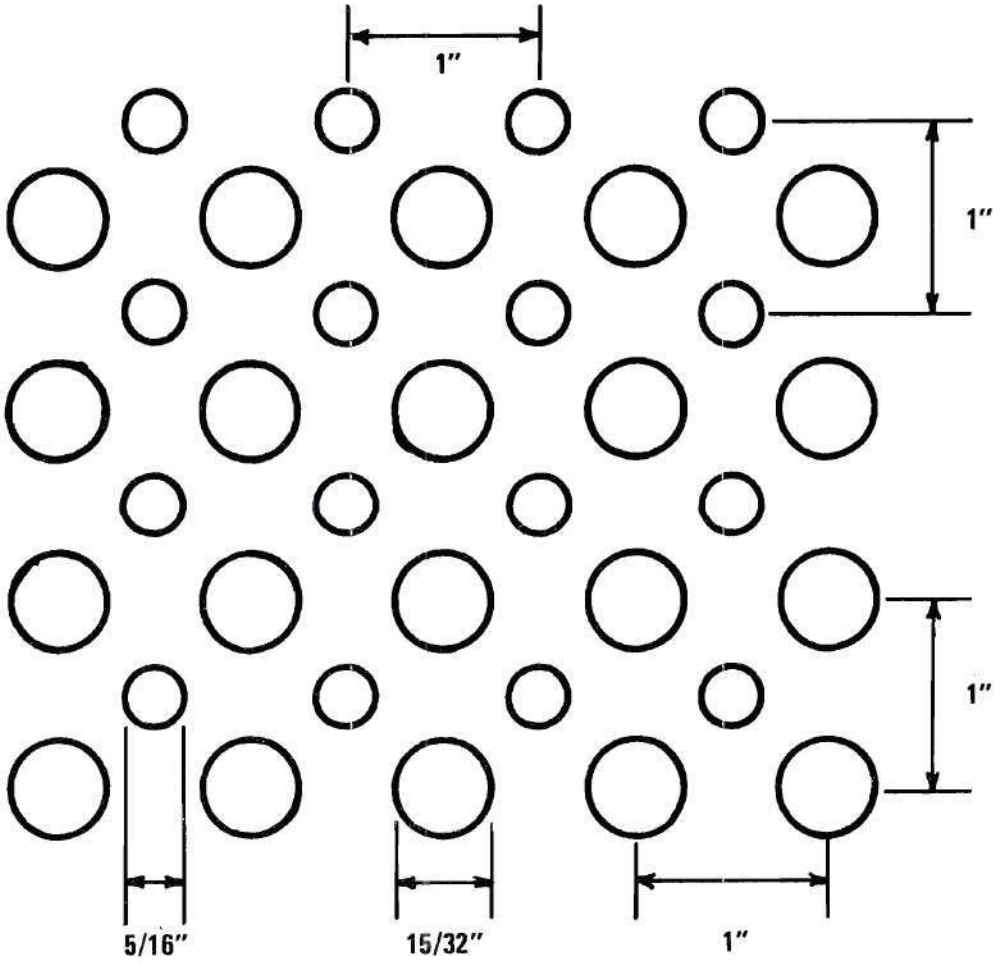

Figure 5. Hole Size and Pattern for Sand Placement Box

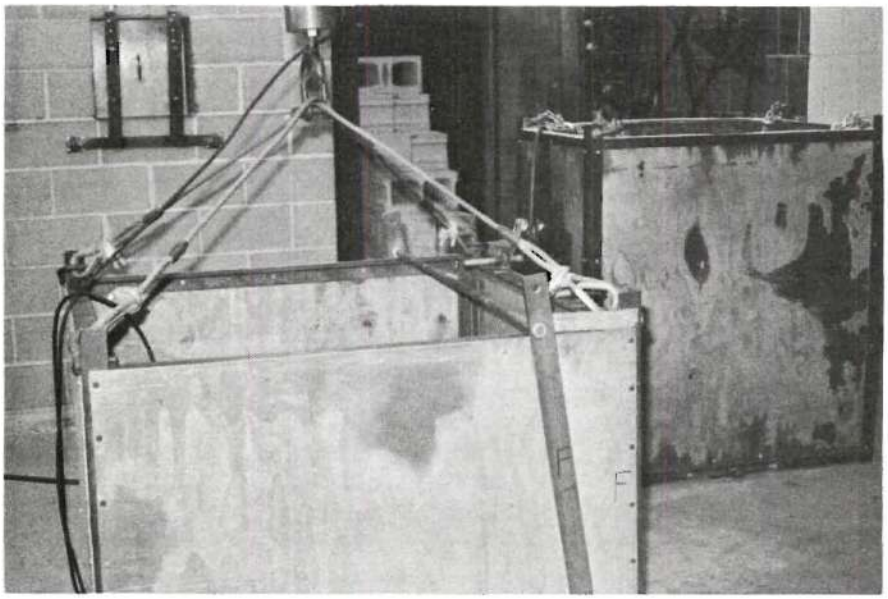

Figure 6. Sand Placement Box and Lever System

of the sand.

The placement apparatus was so constructed that it contained, when full, approximately one-half of the volume of sand needed to fill the test vessel. Wire rope slings were connected to opposite corners of the top of the box to inable the box to be lifted. A 25 kip capacity load cell was attached to the wire rope slings. The load cell was placed in this position to permit the weighing of the placement apparatus at any time. The load cell had a steel eye attached to it to enable the overhead crane to be connected to the load cell when the placement apparatus was to be lifted. The weight of the placement apparatus was determined from the output of the load cell as monitored from the strain indicator box.

Sand Mass Test Bin

The container in which the sand was placed to be tested was constructed using 8" x 8" x 16" concrete blocks. These blocks were fixed into position using masonary cement. Reinforcing wire mesh was placed between each layer of blocks to further strengthen the mortar joint between layers of blocks against lateral deflection. The blocks were laid in an overlapping pattern and aligned such that the hollow cylinders of the blocks formed continuous vertical columns.

To facilitate emptying sand from the test chamber,

the test chamber was constructed above the general floor level. This was done with concrete blocks laid in such a manner so as to give a 48 inch square clear interior. Several interior columns of blocks were used to give added support to the floor of the test bin. The top of the blocks forming the walls and the top of the interior columns were made to be level with respect to each other. After the leveling process, alternate hollow columns of the blocks were filled with a number six steel reinforcing bar and concrete. The reinforcing bar extended approximately eight inches above the top of the concrete blocks. The reinforcing bars and concrete were to further strengthen the walls of the box. Once the hollow columns had been filled, a 5/8 inch thick piece of aluminum sheeting was placed over the blocks to serve as the floor of the test vessel. The aluminum sheeting had holes located around its edge to allow the reinforcing bars to pass through it. After the aluminum sheet was positioned, another six layers of concrete blocks were laid. The same hollow columns of these blocks were filled with reinforcing bars and concrete as were filled for the initial six layers of blocks. Thus there were for all practical purposes continuous reinforced columns for the entire height of the concrete blocks. The hollow columns which were not filled with concrete were filled with sand. This added to the mass of the upper

portion of the test bin and thus aided in resisting any vibrations acting on the concrete blocks.

The final height of the test bin was slightly more than eight feet. However, only the top four feet of the test bin were actually used to hold sand during any test. Thus the bottom of the sand in the test bin was more than four feet above the floor and this height aided in the removal of the sand from the test bin. An opening of 16" x 16" was left in one wall of the blocks just above the aluminum sheet which formed the floor of the sand retaining portion of the test bin. This opening, which was centered in the wall, was to allow for the removal of the sand from the test bin. The opening was sealed during a test by placing a 5/8 inch thick piece of aluminum sheeting into the opening. Figure 7 indicates the concrete block test bin, the door which sealed the test bin, and the mechanism which held the door in position during a test.

Reaction Frame

Figure 8 shows the reaction frame with the loading actuator connected to it. The reaction frame, which provided the resisting force for the actuator when the actuator was loading a specimen, was constructed using 6" x 6" wide flange steel members. The columns (two per side) were 9'10" in height and each was welded to a 12" x 3" piece of steel channel. The steel channel was anchored to the

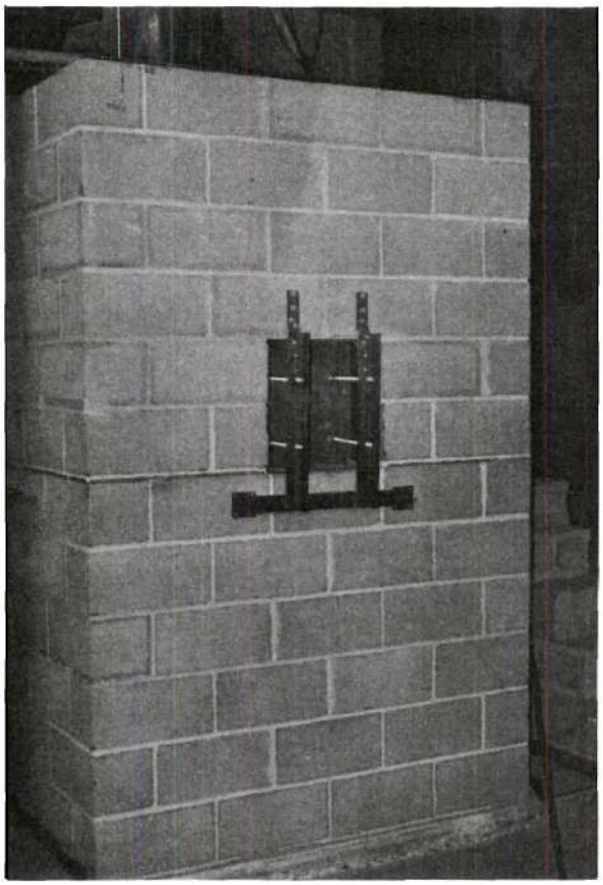

Figure 7. Concrete Test Bin

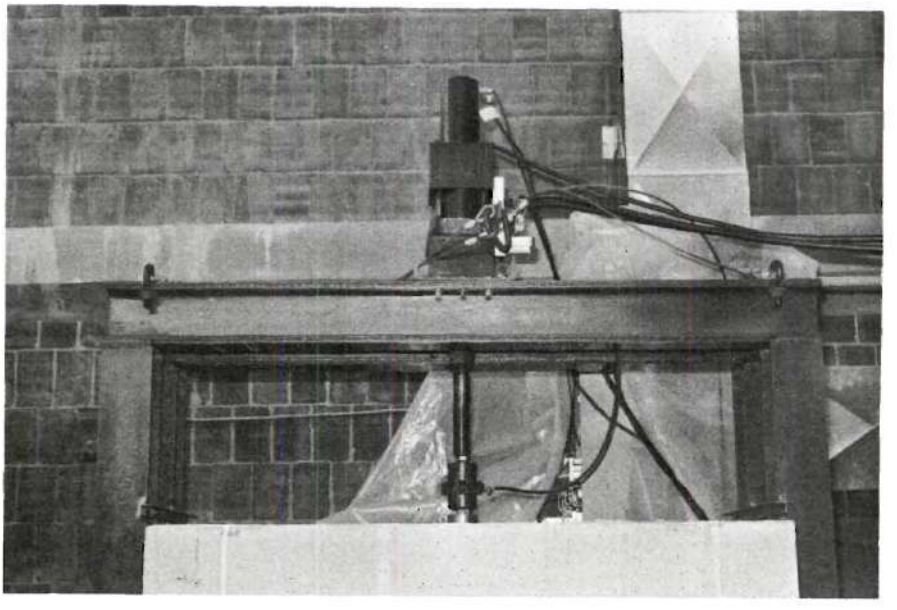

Figure 8. M.T.S. Actuator Reaction Frame

floor using anchor bolts. There were two beams that held the M.T.S. actuator between them. The actuator was bolted to a piece of 12" x 3" steel channel, and this piece of channel was bolted to each of the beams. When a test was to be performed, the two beams were bolted to cover plates on top of the two sets of columns. The two beams holding the actuator were stiffened to strengthen against deflection by welding 6" x 1/2" steel flat stock to both sides of each beam.

Soil Strain Gage Alignment Device

Circular coil inductance type soil strain gages were used to measure movements within the sand mass. In order to accurately place and align these gages in the sand mass, a guide was required. This guide was composed of a frame and alignment device. The frame was bolted to pieces of steel angle which had been welded to the sets of columns of the reaction frame on both sides of the concrete block test bin. The two pieces of aluminum forming the frame passed across the top of the concrete block test bin and these pieces had holes drilled through them at various locations along their length. The alignment device was composed of an aluminum bar and a movable clamping device. The bar fit between the aluminum pieces forming the frame and had pins which fit the holes of the frame at each end of the bar. The alignment device had a clamping apparatus

which could be moved horizontally between the two portions of the frame. The clamping device was constructed so that its horizontal position could be held constant by locking the device in position. Once the horizontal position of the device was fixed, a movable rod was lowered vertically to the desired depth and the position of the soil strain gage was indicated. The alignment device was thus able to insure the axial alignment of any pair of soil strain gages. Figure 9 indicates the alignment device.

Confined Sample Container

A six inch diameter cylindrical piece of seamless steel tubing six inches in length was used as the container for confined sand samples. This container was sealed on one end and had a two inch long extension which could be attached to the open end of the six inch cylinder. This extension permitted sand to be placed into the cylinder to a height of more than the desired six inch sample height.

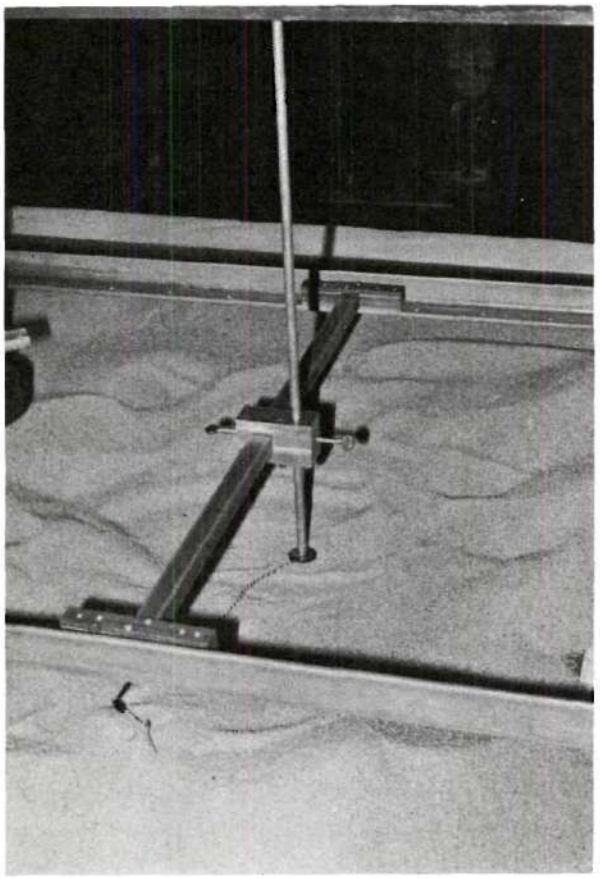

Figure 9. Soil Strain Gage Alignment Frame

CHAPTER VI

INSTRUMENTATION

A M.T.S. closed-loop servo-hydraulic testing system, manufactured by M.T.S. Systems Corporation, Minneapolis, Minnesota, was utilized in loading the sand samples. This system permitted the application of any static load, dynamic load, dynamic load wave form, and frequency to a hydraulic actuator. The actuator used was a model 204.31 with a 50 kip capacity and a six inch stroke limit. The desired combination of the above functions was applied with the hydraulic actuator to the sand mass.

Connected to the movable ram of the hydraulic actuator were a linear variable differential transducer (LVDT), load cell, and a circular loading plate. The LVDT, model made by G. L. Collins Corporation, Long Beach, California, was internally mounted in the top of the hydraulic actuator. In this position it was used to monitor settlement of the movable ram and also the amplitude of vibration of the ram during dynamic loading; resolution to at least 0.0001 was possible with this LVDT. To measure contact force a load cell was used; the model employed was a BLH Electronics Inc., Waltham, Massachusetts model C3P2B with a three millivolt per volt output. This cell had a

capacity of ten kips. Using the amplifiers in the M.T.S. system, the load cell output could be resolved to within approximately ± two pounds. This load cell had an accuracy of 0.10% with a maximum hysteresis of 0.05%. The load cell was positioned at the bottom of the movable actuator ram and connected to the ram through a threaded steel adaptor. Connected to the bottom of the load cell with a steel threaded adaptor was a circular loading plate. This loading plate was machined from 1.5 inch thick steel stock. The plate was five inches in diameter. The plate was assumed thick enough to act as a rigid plate. Figure 10 shows the connection of the loading plate to the load cell and the connection of the load cell to the movable ram of the M.T.S. actuator.

The output of both the load cell and the LVDT was continuously recorded on a model Mark 280 Recorder, manufactured by Brush Instruments Division, Clevite Corporation, Cleveland, Ohio. This recorder gave a continuous record of each test and also provided time marks every second on the paper.

In order to observe the phase angle between the contact force and the amplitude of vibration of the loading plate, a Tektronix model 502A Dual Beam Oscilloscope, made by Tektronix, Inc., Beaverton, Oregon, was used. Photographs of the Lissajous figures produced on the

Figure 10. Load Cell and Loading Plate

oscilloscope were taken using a Hewlett-Packard Poloroid Scope Camera.

To monitor the vertical vibrations of the steel loading plate without the movement of the load frame being measured, a G. L. Collins 203 LVDT (range = 0.125 inches and accurate to $\pm$ 0.0001 inch) was positioned against the plate. A G. L. Collins DCR-301 model 24 volt stabilized D.C. power supply was used to excite the LVDT, and the output was monitored on a Sanborn Model 320 Dual Channel D.C. Amplifier-Recorder, manufactured by Hewlett-Packard, Sanborn Division, Waltham, Massachusetts.

To weigh the amount of sand contained in the test vessel, a model S/N FLU-25SP2-0210 single bridge Universal Flat Load Cell with a two millivolt per volt output and an accuracy of 0.03% on loading was used. This load cell was manufactured by Strainsert Company, Bryn Mawr, Pennsylvania. The output of the load cell was monitored on a model 120C Strain Indicator, made by BLH Electronics Inc., Waltham, Massachusetts.

To observe the movement within the sand mass, several sets of Bison Soil Strain Gages, manufactured by Bison Instruments Inc., Needham Heights, Massachusetts, were placed within the sand mass. The separation of any two sensors was related to the electro-magnetic coupling between the two sensors. By means of an external inductance

bridge, an output voltage as a function of the separation of the sensors was obtained for any position of the gages. Movements of $\pm$ 0.001 inches were able to be monitored with these gages. Appendix B contains the complete description and calibration procedure for these gages.

CHAPTER VII

PROCEDURE FOR UNCONFINED SAMPLES

Pre-Test Procedure

Sand and Soil Strain Gage Placement

In order to perform tests on a quantity of sand at a given density, a reproducible method of placing the sand uniformly over an area was required. Kolbuszewski (19), by conducting very small experimental tests, concluded that for a dry sand a wide range of porosities (therefore densities) could be obtained by permitting sand to fall or rain to form a uniform bed. Walker and Whitaker (46) and Brumund (4) used this raining technique to form large beds of sand that were uniform in density. Therefore, the method selected was that of "raining" the sand over the desired area. This "raining" method depended on giving sand particles enough energy so that on impact with a surface the sand particles would pack together to form a uniform mass (achieve a minimum potential energy state). By varying the intensity of placement and initial energy of the sand particles, the denseness of the uniform mass could be varied. The intensity of placement could be varied by changing the quantity of sand being "rained" upon the surface. The intensity of flow of the sand influenced the

amount of particle interference with other particles and thus affected the final energy of the particles. The initial energy of the sand could be varied by changing the distance the sand could fall. Thus, by adjusting the intensity of sand being "rained" out of a container and the height of fall of the sand, any possible density for the sand could be obtained. For any constant height of fall, the maximum density of the sand mass was obtained by "raining" the sand onto the surface at a very slow rate while the minimum density was obtained using a very fast or high rate of flow. By adjusting the height of fall "the" maximum and minimum densities could be obtained.

To achieve this "raining" method, the sand placement apparatus or box was used. The box was filled with sand and then the box was lifted over the concrete block test bin using the overhead crane. Before the box was lowered into the test bin, the weight of the box and sand was measured. This was accomplished by connecting the electrical leads of the load cell which connected the box to the crane to a strain indicator box and recording the output of the load cell as indicated on the strain indicator box. After the weight was obtained from a load-strain calibration curve, the box was lowered into the concrete block test bin. The desired mass density for the sand was selected and this determined the degree of alignment between the two plates

of the sand placement apparatus. Appendix C gives the method which was used to correlate the sand density and the position of the open-close lever of the sand placement box. After the desired density was selected, the stop bolts on the sand placement box were set to the required position as determined from Figure 34 of Appendix C. With the stop bolts positioned and the box lowered into the concrete block test bin to a position that gave the correct height of fall to the sand, the open-close lever of the box was opened until it struck the stop bolts of the box. As the sand flowed out of the box, the box was slowly raised in order to keep the height of fall of the sand at approximately the correct distance. Once all the sand had flowed out of the box, the weight of the empty box was determined using the load cell and strain indicator box. The box was then lowered back onto the floor where the crane was disconnected from the sand box. The crane was next connected to a second container which held the remainder of the sand required to fill the concrete block test bin. The second box was raised over the sand placement box and a trap door in the bottom of the second box was opened to allow the sand to flow from that box into the sand placement box. After the second box had been emptied, it was lowered back to the floor and the crane was disconnected. The crane was reconnected to the sand placement box, and this box was

lifted over the concrete block test bin and its weight determined as was done initially. Before the remaining sand was rained into the test bin, the soil strain gage placement frame was positioned. The initial strain gage was placed on the surface of the sand using the alignment device attached to the frame. After the gage was positioned, a bubble level was used to insure that the gage was level. The alignment device and placement frame were then removed and the sand raining process was started and continued until the desired amount of sand above the soil strain gage was reached. At this point, the flow of sand was stopped and the process of placing another strain gage was repeated. The alternate processes of raining sand into the test bin and placing the soil strain gages were continued until the last strain gage was in position. The depth between the finished surface of the sand and the last gage was measured from the bottom of the screeding bar. After this depth was measured, the test bin was overfilled with sand. The overfilling of the test bin was to insure that the entire finished surface of the test bin was covered with sand which had been rained onto it from the placement box. With the test bin overfilled, the weight of the sand placement box and any sand remaining in the box was measured in the same manner as before.

The finished surface of the sand was obtained by

screeding the excess sand off of the test bin. This was accomplished by moving an aluminum bar which was longer than the width of the test bin over the surface of the concrete blocks. Thus the final surface of the sand corresponded to the surface of the concrete blocks. The excess sand from the screeding process was returned to the sand placement box, and the box with the sand was weighed. With this final weighing, the amount of sand placed into the test bin could be calculated, and thus the density of the sand mass could also be calculated. Sample calculations are shown in Appendix D.

Reaction Frame and Vibration Monitor Placement

Once the sand was in the test bin and the final weighing of the sand placement box had been finished, the sand placement box was lowered to the floor where the overhead crane was disconnected. The crane was then connected to the beams which held the M.T.S. actuator. The beams were raised and placed on top of the steel frame columns of the reaction frame. The beams were then bolted to the columns of the frame using four bolts per column. After the beams were bolted to the columns, the LVDT which monitored the plate vibration during any load application of the M.T.S. ram was positioned. In this position, the amplitude of vibration of the plate during a test could be monitored. The vertical position of the LVDT was adjusted

until the output of the LVDT could be monitored by a Hewlett-Packard recorder.

Initial Soil Strain Gage Readings

The final step to be completed before the test was initiated was the recording of the initial output of the soil strain gage pairs. The null amplitude readings for each pair of gages were recorded. The gages were placed within the sand in such a manner that an inductance could be measured between any two gages. Figure 11 indicates the usual positioning of the gages within the sand mass and the different pairs of gages that could be monitored.

Test

With the sand "rained" into the test bin, the M.T.S. actuator in position, and the initial readings of the soil strain gages recorded, the M.T.S. equipment was energized. The M.T.S. ram was slowly lowered to place the circular loading plate just into contact with the sand surface. As the loading plate was lowered into position, the pen on the load monitoring channel of the Mark 280 Brush recorder was adjusted to a null or zero position. The scales of both channels, one monitoring load and one monitoring movement, of this recorder were then positioned to their desired levels. At this time, the 24 volt D.C. power supply exciting the external LVDT measuring plate movement and the Hewlett-Packard recorder monitoring the external LVDT were

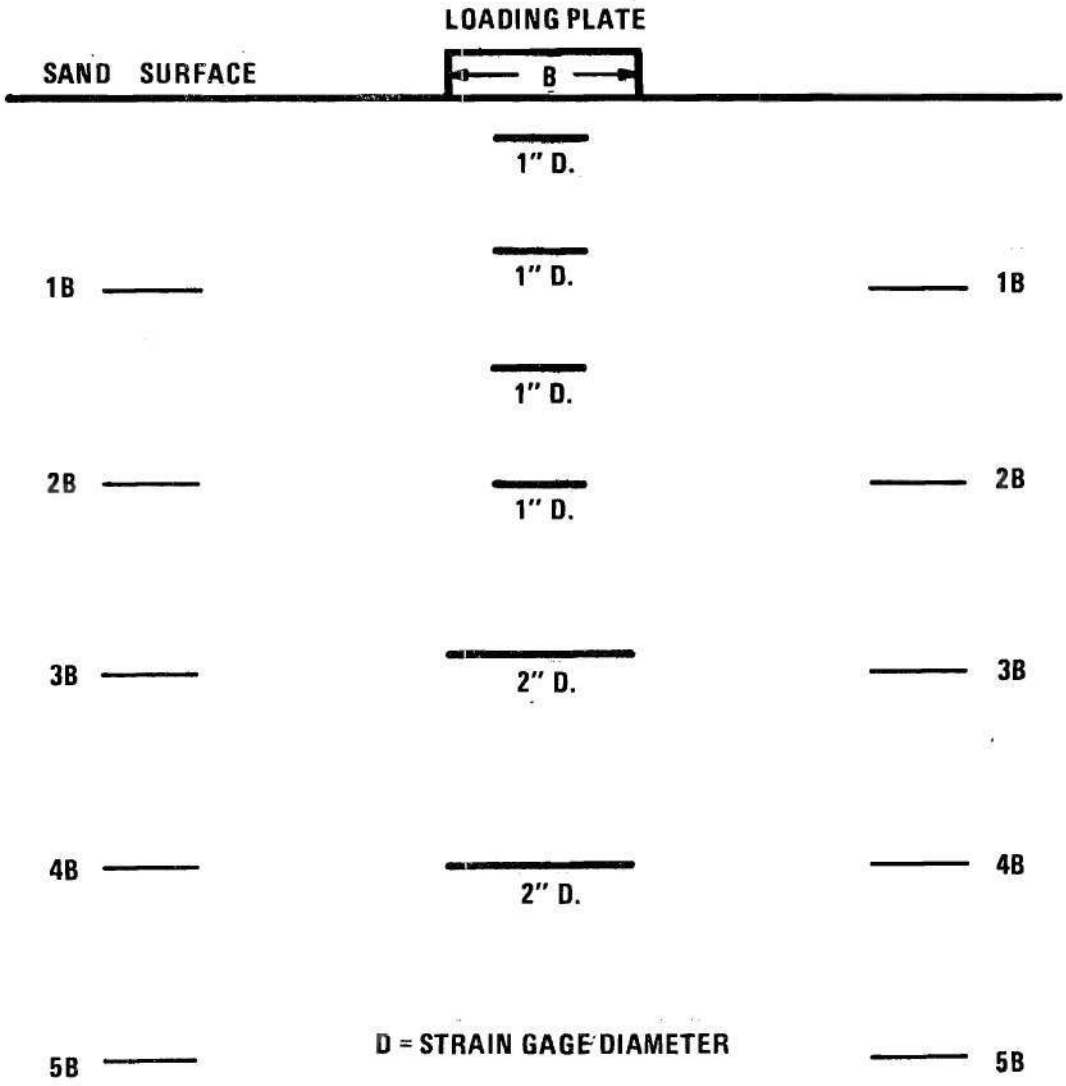

Figure 11. Soil Strain Gage Positioning

switched on. After placing the recorders at the proper settings, the selected static load was applied to the sand mass through the loading plate and M.T.S. ram. This load remained on the sand throughout the remainder of the test. The completion of the static settlement was determined by monitoring the settlement on the Mark 280 recorder. The dynamic load was only applied after all the settlement of the loading plate due to the applied static load had ceased. Once the static settlement ceased, the dynamic loading, in the form of a sinusoidal wave, was applied to the sand mass. With the M.T.S. equipment, the dynamic loading could not be applied instantaneously. It required approximately six seconds to adjust the M.T.S. system to obtain the selected loading. With the dynamic loading applied to the sand mass, the load settlement was continuously monitored on the Mark 280 recorder for the entire length of the test. The equipment monitoring the plate vibrations was turned off after the first 30 seconds of the dynamic load application and then turned back on for the final 30 seconds of the test. The dynamic loading on the sand was continued for 60 minutes for the standard test. Before the loads were removed from the sample, a photograph of the Lissajous figure produced on the oscilloscope by monitoring load versus amplitude of plate vibration was taken. After the 60 minutes of load application, both the dynamic and static loads were

removed from the sand mass. This completed the loading portion of the test.

Once the loading of the sand mass had been completed, final readings of the soil strain gages were recorded. To obtain the complete set of gage movement readings, the beams holding the M.T.S. actuator were disconnected from the reaction frame columns and the beams and actuator were lowered to the floor. The sand above the top strain gage was carefully excavated. The strain gage frame and alignment device were positioned and the depth from the bottom of the screeding bar down to the top of the strain gage was measured. This final measurement completed the test.

CHAPTER VIII

PROCEDURE FOR CONFINED SAMPLES

Sand Placement

The confined sample container with its two inch extension attached was placed on a level stand. The desired relative density of the sand for the test was selected. With the relative density selected, the sand was "rained" into the container using a funnel with a wire mesh bottom to diffuse the sand as it struck the mesh. The sand was poured through the funnel with the rate of flow and height of fall for the sand being varied according to the desired density. The container was filled with sand, and then the two inch extension was removed. The surface of the sand was then leveled off flush with the top of the container giving a sand sample height of six inches. The container and sand were then weighed to determine the actual relative density of the sand.

Test

With the sand in the container at the desired relative density, the container was placed upon a loading platform under the M.T.S. actuator. The six inch diameter loading plate attached to the actuator was then lowered

into contact with the sand surface. A static load was chosen for the test and applied to the sand sample. The loading plate was allowed to reach an ultimate settlement under the static load application. After the ultimate static settlement was reached, a selected dynamic load and frequency of load application were then applied to the sand. All loads, amplitudes of vibration, and settlements were continuously monitored. The dynamic portion of the test was continued for 60 minutes. The amplitude of vibration of the plate at the end of the test and the final settlement of the plate were recorded.

CHAPTER IX

TEST PROGRAM

In order to determine the validity of the hypotheses proposed in this study, the following test program was followed.

In order to determine the load limits which could be used during dynamic testing, static load tests were conducted. These tests were performed on the sand placed at each of the four relative densities that were to be used in the dynamic test program.

To establish the vibration wave reflection characteristics of the test bin at several different relative densities, tests were performed with the test bin lined and unlined. These tests were run using a frequency of 30 Hz. At a relative density of approximately 71 percent tests were also performed at frequencies of 30 Hz., 40 Hz., and 50 Hz. with the test bin lined and unlined.

The standard test program on unconfined samples (loaded area small in comparison to total surface area) consisted of placing the sand in the lined test bin at one of four relative densities. Then a static and dynamic load combination below the static bearing capacity of the sand was applied to the five inch diameter loading plate. For

all the tests performed at relative densities other than 71 percent, the dynamic frequency was maintained at 30 Hz. At the relative density of 71 percent, the frequency was varied between 30 Hz. and 70 Hz.

Finally, for unconfined sand samples at a relative density of approximately 71 percent tests were performed at various frequencies with soil strain gages placed within the sand mass.

Confined sample (entire sample surface loaded) tests were performed at relative densities of 49, 70 and 82 percents. The frequency of vibration for this series of tests was 30 Hz.

CHAPTER X

RESULTS

Static Load Tests

Figure 12 indicates the load-deflection characteristics for the five inch loading plate under static loading conditions. The relative densities of the sand for these static tests were 22, 55, 71, and 82 percent respectively. From these tests, the ultimate capacity at each of the above relative densities was found to be approximately 200, 450, 650, and 700 pounds for the five inch diameter plate (corresponding to bearing capacities of 10.2 psf, 23.0 psf, 33.2 psf, and 35.7 psf).

Test Duration

The effect of length of vibration time on the normalized settlement of the plate is indicated in Figure 13. The results of four different tests on unconfined samples and one for a confined sample, which are representative of all the tests, are shown. The relative density for all of these tests was approximately 70 percent. Two tests were performed on the unconfined samples and one on the confined sample using a frequency of 30 Hz., while the static and dynamic loadings were different. Two other tests on the

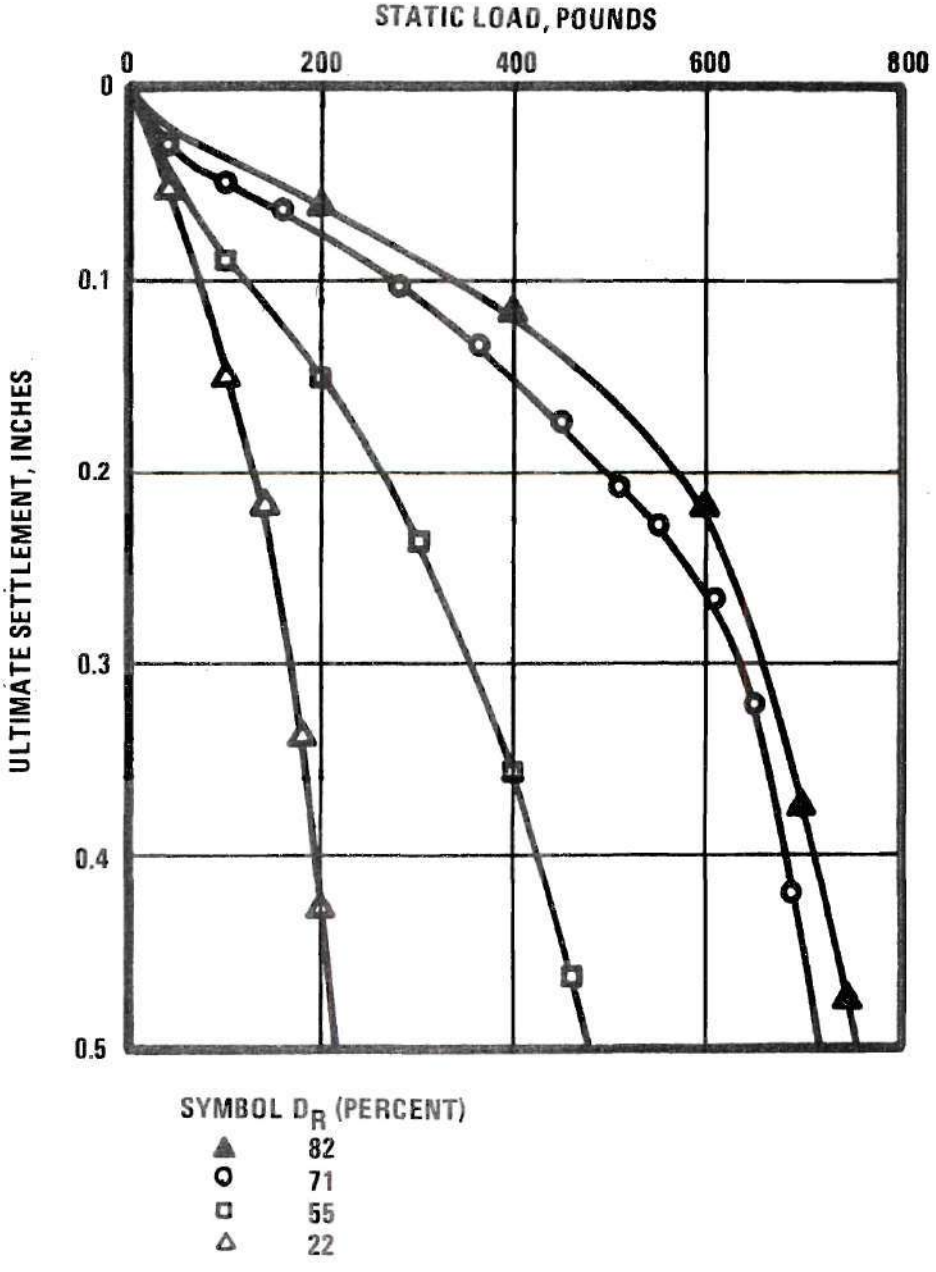

Figure 12. Static Load Tests

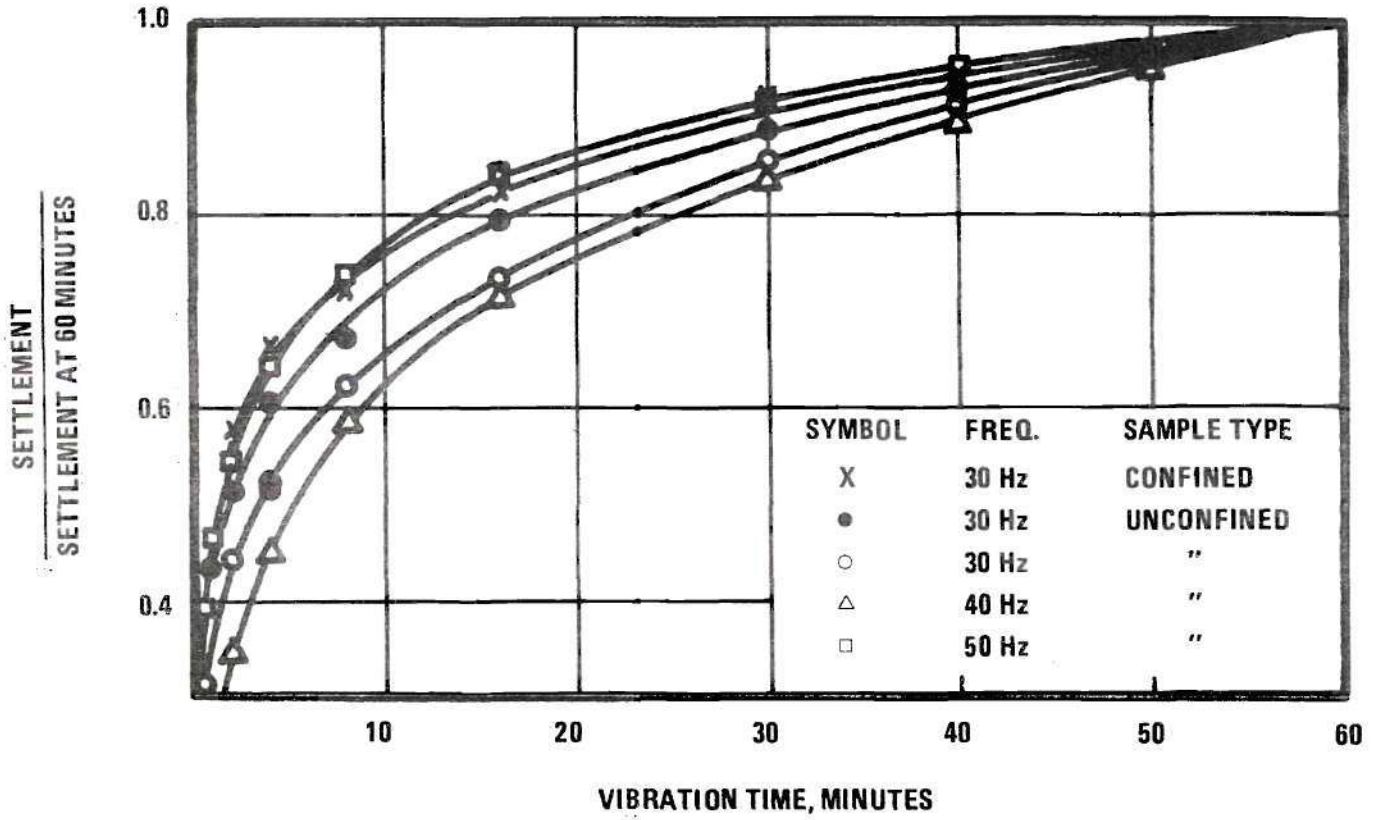

Figure 13. Normalized Plate Settlement vs Vibration Time

dynamic loadings were different. Two other tests on the unconfined samples were performed at frequencies of 40 and 50 Hz. with loading conditions for each which did not coincide with those of the other tests. The curves for the various tests all indicate that the rate of change of settlement with time after 60 minutes is very small and that the system is almost in equilibrium under a steady-state input. The logarithm of time-settlement curves for the four individual unconfined sample tests are shown in Figure 14; Figure 15 gives the same curve for the confined sample.

Effects of Test Bin Vibration Wave Reflection on Unconfined Tests

In order to observe the effects of wall wave reflection, tests were run with the walls of the test bin bare (concrete block walls), and with the walls of the test bin lined with one inch thick polyurethane. At each of the four test densities, tests were performed at approximately the same steady-state transmitted energy levels with the test bin walls bare and with the test bin walls lined. The results of these tests are shown in Table 1. The effects of the two wall conditions on the settlement of the loading plate for two frequencies of vibration were determined at a relative density of 71 percent. These results are also shown in Table 1.

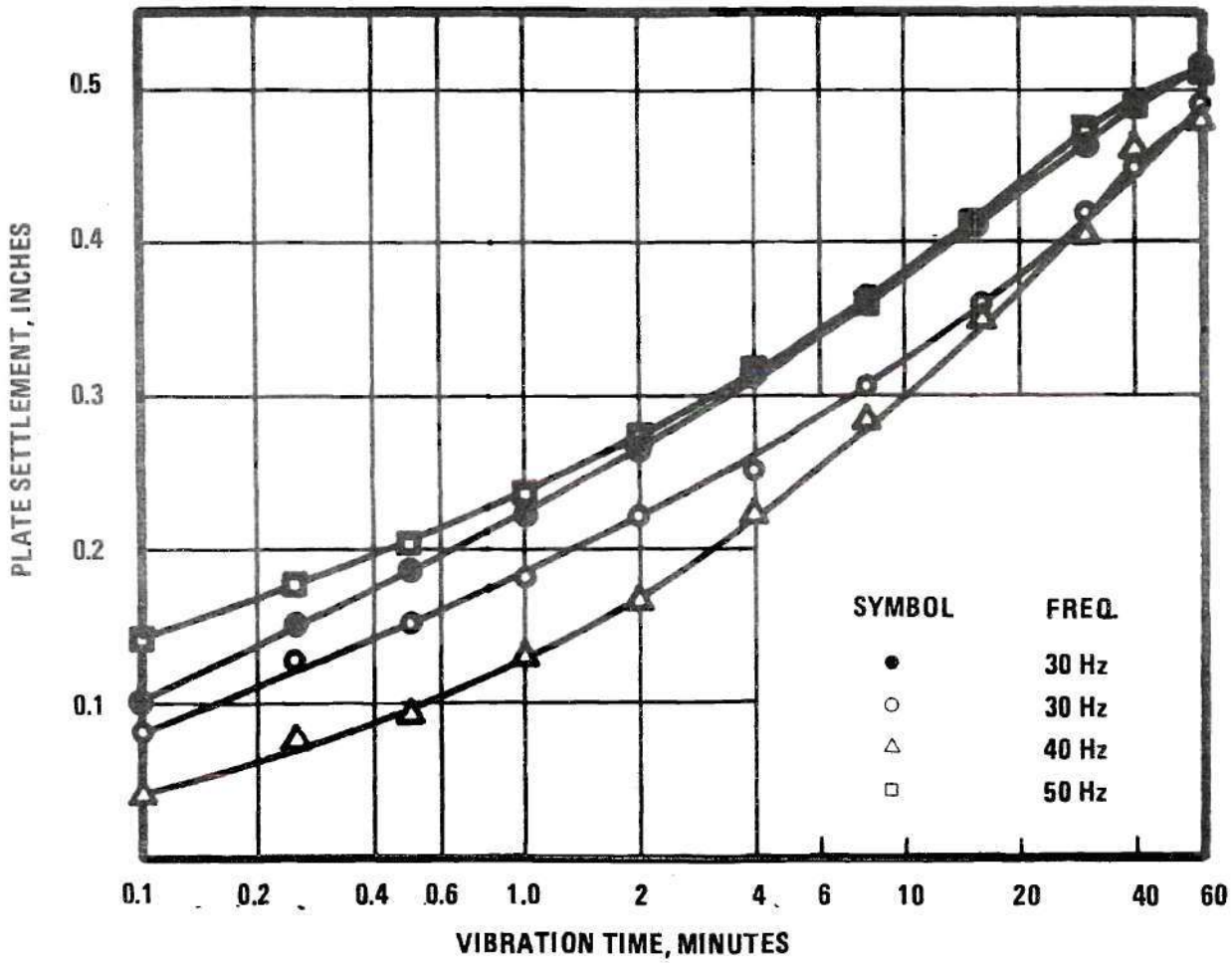

Figure 14. Plate Settlement vs Logarithm of Vibration Time for Unconfined Samples

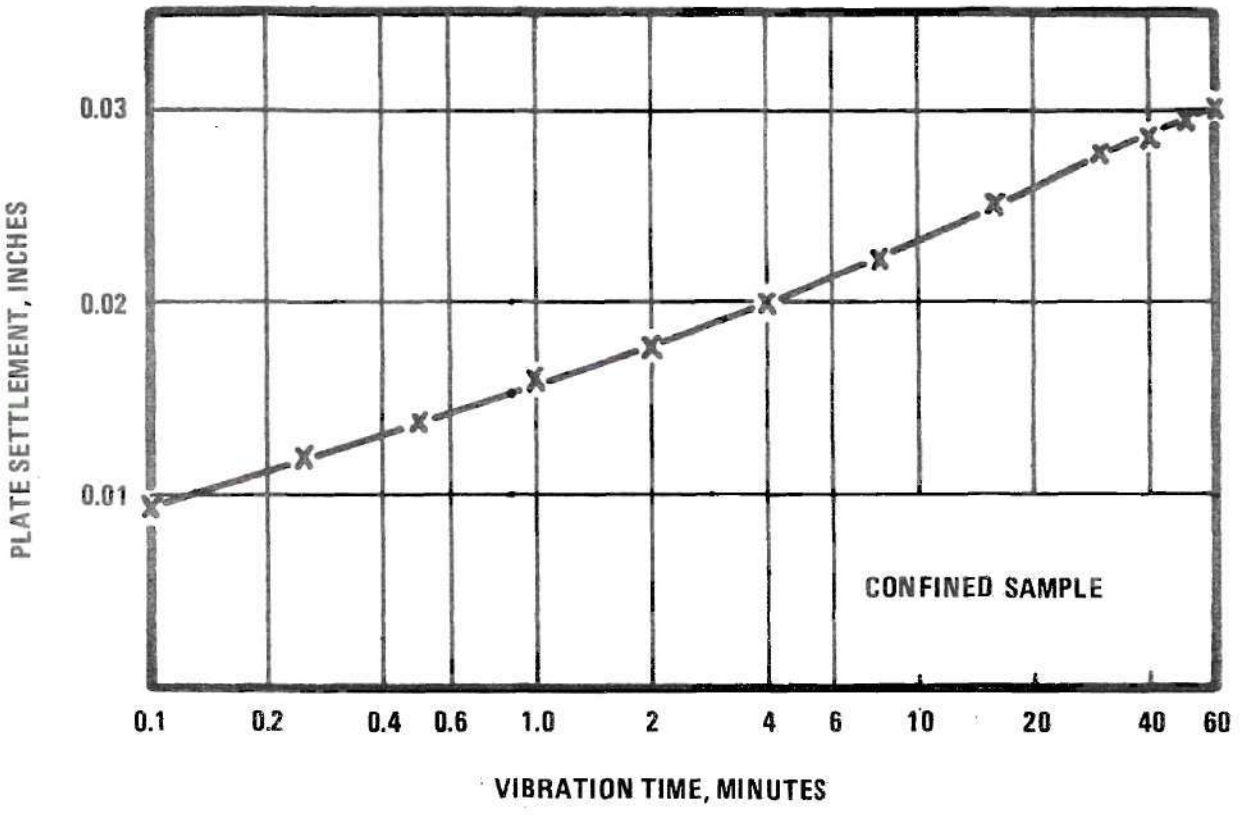

Figure 15. Plate Settlement vs Logarithm of Vibration Time

Table 1. Results of Tests
Performed in Lined and Unlined Test Bin

Test No.	D_R (%)	Freq. (Hz)	Static Load (lbs)	Dynamic Load (lbs)	S_{60} Lined (inches)	S_{60} Unlined (inches)
105	72.4	30	100	60	0.218	
33	68.2	30	100	60		0.301
101	42.0	30	150	80	1.000	
65	44.4	30	150	80		1.236
100	27.2	30	100	60	0.815	
69	23.0	30	100	60		0.983
103	80.4	30	100	60	0.170	
*	82.0	30	100	60		0.201*
96	65.2	50	200	100	0.705	
79	71.6	50	200	100		1.193

* Extrapolated values from tests.

Tabulated Results of Unconfined Sample Test Program

The following tables summarize the results of the tests performed on unconfined samples.

1) Table 2 Average D_R = 22 percent
2) Table 3 Average D_R = 51 percent
3) Table 4 Average D_R = 71 percent
4) Table 5 Average D_R = 82 percent
5) Table 6 Soil Strain Gage Data

Tests one through 95 were performed in the unlined test bin. Spurious wave reflections were found to be affecting the settlements of the vibrating plate; therefore, the test bin was lined for all tests 96 and above. The values of settlement for the tests one through 95 were modified to account for the wave reflection problem, and the modified values are shown in the tables. The modification was made by applying reduction factors to the settlements of the tests performed in the unlined test bin. The reduction factor for each relative density was determined from performing replicate tests in the lined and unlined test bin. At relative densities of 22, 51, and 82 percent, the frequency for the replicate tests was 30 Hz., while at 71 percent relative density the various frequencies were used.

Plate Settlement-Transmitted Energy Relationship

At each of the relative densities of 22, 51, 71 and 82 percent, different static and dynamic load combinations

Table 2. Results of Unconfined Sample Tests
With an Approximate Relative Density of 22 Percent

Test No.	D_R (%)	Freq. (Hz)	Static Load (lbs)	Dynamic Load (lbs)	$A_P \times 10^3$ (inches)	E_{TR} (in-lbs)	S_{60} (inches)
66	34.4	30	100	40	1.55	0.155	0.525
68	20.8	30	95	40	1.90	0.180	0.612
69	23	30	100	60	2.45	0.245	0.825
71	23.8	30	50	20	0.90	0.045	0.185

Table 3. Results of Unconfined Sample Tests
With an Approximate Relative Density of 51 Percent

Test No.	D_R (%)	Freq. (Hz)	Static Load (lbs)	Dynamic Load (lbs)	$A_p \times 10^3$ (inches)	E_{TR} (in-lbs)	S_{60} (inches)
40	51.8	30	100	40	0.735	0.074	0.130
41	47.0	30	150	40	0.604	0.091	0.180
43	48.2	30	150	80	1.312	0.197	0.500
44	47.6	30	150	120	2.045	0.307	0.711
45	52.8	30	50	20	0.420	0.021	0.061
47	52.4	30	200	80	1.629	0.326	0.671
48	51.2	30	200	60	1.160	0.232	0.620
49	49.6	30	200	120	2.360	0.472	1.027

Table 4. Results of Unconfined Sample Tests With an Approximate Relative Density of 71 Percent

Test No.	D_R (%)	Freq. (Hz)	Static Load (lbs)	Dynamic Load (lbs)	$A_p \times 10^3$ (inches)	E_{TR} (in-lbs)	S_{60} (inches)
24	70.6	30	250	200	4.935	1.234	1.681
26	68.2	30	250	100	1.990	0.499	0.673
28	74.0	30	250	125	2.520	0.630	0.937
29	69.2	30	200	120	2.730	0.546	0.676
30	69.2	30	200	80	1.470	0.294	0.414
31	71.0	30	200	40	0.840	0.168	0.161
32	70.0	30	100	80	2.950	0.295	0.348
33	68.2	30	100	60	2.250	0.225	0.249
34	70.0	30	100	40	1.310	0.131	0.116
75	68.6	35	200	100	2.500	0.500	0.709
76	68.6	40	200	100	3.780	0.757	1.030
77	67.6	50	200	100	2.030	0.405	0.690
78	70.6	30	200	100	2.520	0.504	0.651
79	71.6	50	200	100	1.640	0.328	0.596
80	64.0	50	200	100	1.800	0.360	0.576
82	70.6	45	200	100	6.600	1.320	1.738

Table 4. (Continued)

Test No.	D_R (%)	Freq. (Hz)	Static Load (lbs)	Dynamic Load (lbs)	A_p X 10^3 (inches)	E_{TR} (in-lbs)	S_{60} (inches)
88	65.8	45	100	50	2.900	0.290	0.456
95	70.0	70	200	100	2.660	0.533	0.813
96	65.2	50	200	100	1.590	0.318	0.705
97	76.0	30	200	100	2.670	0.534	0.649
104	76.4	40	100	60	3.070	0.307	0.349
105	72.4	30	100	60	1.890	0.189	0.218
106	74.5	50	150	80	1.632	0.245	0.512
107	75.0	40	150	80	3.580	0.537	1.971
108	71.0	40	100	60	2.850	0.285	0.784
109	71.0	30	100	75	3.750	0.375	0.516
110	72.8	30	100	75	2.570	0.257	0.466
111	62.4	30	100	80	3.090	0.309	0.549
112	68.0	50	150	80	1.648	0.247	0.658
113	64.8	40	100	50	2.480	0.248	0.474
114	69.0	30	100	80	2.980	0.298	0.490
116	70.0	45	100	50	1.930	0.193	0.329

Table 5. Results of Unconfined Sample Tests With an Approximate Relative Density of 82 Percent

Test No.	D_R (%)	Freq. (Hz)	Static Load (lbs)	Dynamic Load (lbs)	$A_p \times 10^3$ (inches)	E_{TR} (in-lbs)	S_{60} (inches)
57	86.0	30	250	125	2.780	0.695	0.720
58	76.6	30	50	30	0.789	0.039	0.041
59	85.2	30	300	200	4.570	1.370	1.365
61	79.6	30	250	125	2.575	0.643	0.605
102	80.0	30	100	60	1.400	0.140	0.160
103	80.4	30	100	60	1.650	0.165	0.170

Table 6. Soil Strain Gage Separations

Test No.	106		107		108		109	
	Initial	Final	Initial	Final	Initial	Final	Initial	Final
Surface-Gage 1 Separation*	5.008	5.113	4.820	5.066	4.723	4.912	5.085	5.197
Gage 1-2(C.S.)**	3	3	3	3	3	3	3	3
Amplitude***	816	803	798	744	885	843	674	647
Separation	3.034	3.008	2.998	2.898	3.176	3.088	2.776	2.731
Gage 2-3(C.S.)	3	3	3	3	3	3	3	3
Amplitude	603	581	741	714	647	630	770	760
Separation	2.669	2.637	2.891	2.845	2.733	2.707	2.945	2.926
Gage 3-4(C.S.)	3	3	3	3	3	3	3	3
Amplitude	876	871	753	737	796	782	525	521
Separation	3.156	3.146	2.915	2.885	2.996	2.967	2.569	2.566
Gage 4-5(C.S.)	3	3	2	2	2	2	3	3
Amplitude	290	286	418	405	368	360	339	336
Separation	2.273	2.269	2.404	2.390	2.351	2.341	3.404	3.401
Gage 5-6(C.S.)	2	2	2	2	3	3	3	3
Amplitude	379	377	764	761	517	514	15	10
Separation	5.298	5.290	4.790	4.750	5.631	5.623	4.665	4.660

* Gage Separation in Inches

** C.S. = Coil Separation Range

*** Amplitude Dial Readings

Gage Size: Gages 1, 2, 3, and 4 - 1" Diameter
Gages 5 and 6 - 2" Diameter

Table 6. (Continued)

Test No.	110		111		112		113	
	Initial	Final	Initial	Final	Initial	Final	Initial	Final
Surface-Gage 1 Separation	5.057	5.118	3.119	3.278	1.062	1.608	0.917	1.292
Gage 1-2(C.S.)	3	3	3	3	3	3	3	3
Amplitude	599	570	370	272	649	355	815	709
Separation	2.661	2.624	2.410	2.329	2.738	2.398	3.033	2.836
Gage 2-3(C.S.)	3	3	3	3	3	3	3	3
Amplitude	592	582	410	372	752	705	638	595
Separation	2.652	2.639	2.447	2.413	2.913	2.829	2.720	2.656
Gage 3-4(C.S.)	3	3	3	3	3	3	3	3
Amplitude	701	689	836	823	806	787	764	751
Separation	2.820	2.801	3.072	3.048	3.016	2.977	2.934	2.910
Gage 4-5(C.S.)	3	3	3	3	3	3	3	3
Amplitude	593	588	726	718	883	877	942	937
Separation	3.772	3.764	4.047	4.028	4.507	4.485	4.743	4.720
Gage 5-6(C.S.)	2	2	3	3	3	3	3	3
Amplitude	714	709	169	165	561	555	427	420
Separation	4.260	4.240	4.899	4.892	5.756	5.741	5.406	5.392

Table 6. (Continued)

Test No.	114		116	
	Initial	Final	Initial	Final
Surface-Gage 1 Separation	0.787	1.120	1.425	1.645
Gage 1-2(C.S.)	3	3	3	3
Amplitude	839	737	766	682
Separation	3.081	2.885	2.937	2.789
Gage 2-3(C.S.)	3	3	3	3
Amplitude	780	753	711	685
Separation	2.964	2.915	2.839	2.795
Gage 3-4(C.S.)	3	3	3	3
Amplitude	866	856	632	630
Separation	3.136	3.106	2.710	2.706
Gage 4-5(C.S.)	3	3	3	3
Amplitude	951	948	970	961
Separation	4.784	4.773	4.881	4.833
Gage 5-6(C.S.)	3	3	3	3
Amplitude	582	582	406	406
Separation	5.821	5.821	5.358	5.356

were applied to unconfined sand samples, and the settlement after 60 minutes due to these load applications was measured. For each of the densities, a linear relationship between settlement at 60 minutes and steady-state transmitted energy per cycle of loading was determined; these data are shown in Figure 16. To show the influence of frequency, Figure 17 shows the data from Figure 16 at 71 percent relative density with each frequency indicated by a different symbol. The sensitivity of settlement to relative density is shown in Figure 18; this figure shows the ratio of settlement of any relative density to settlement at a relative density of 82 percent as a function of relative density.

Tabulated Results of Confined Sample Test Program

The tables listed below summarize the results of tests performed on confined samples:

1) Table 7 Average D_R = 49 percent
2) Table 8 Average D_R = 70 percent
3) Table 9 Average D_R = 82 percent

Confined Sample Tests

Figure 19 indicates the relationships between normalized settlement (settlement divided by the original sample height) and steady-state transmitted energy per load cycle for various initial sand relative densities. The relative densities at which these tests were performed were

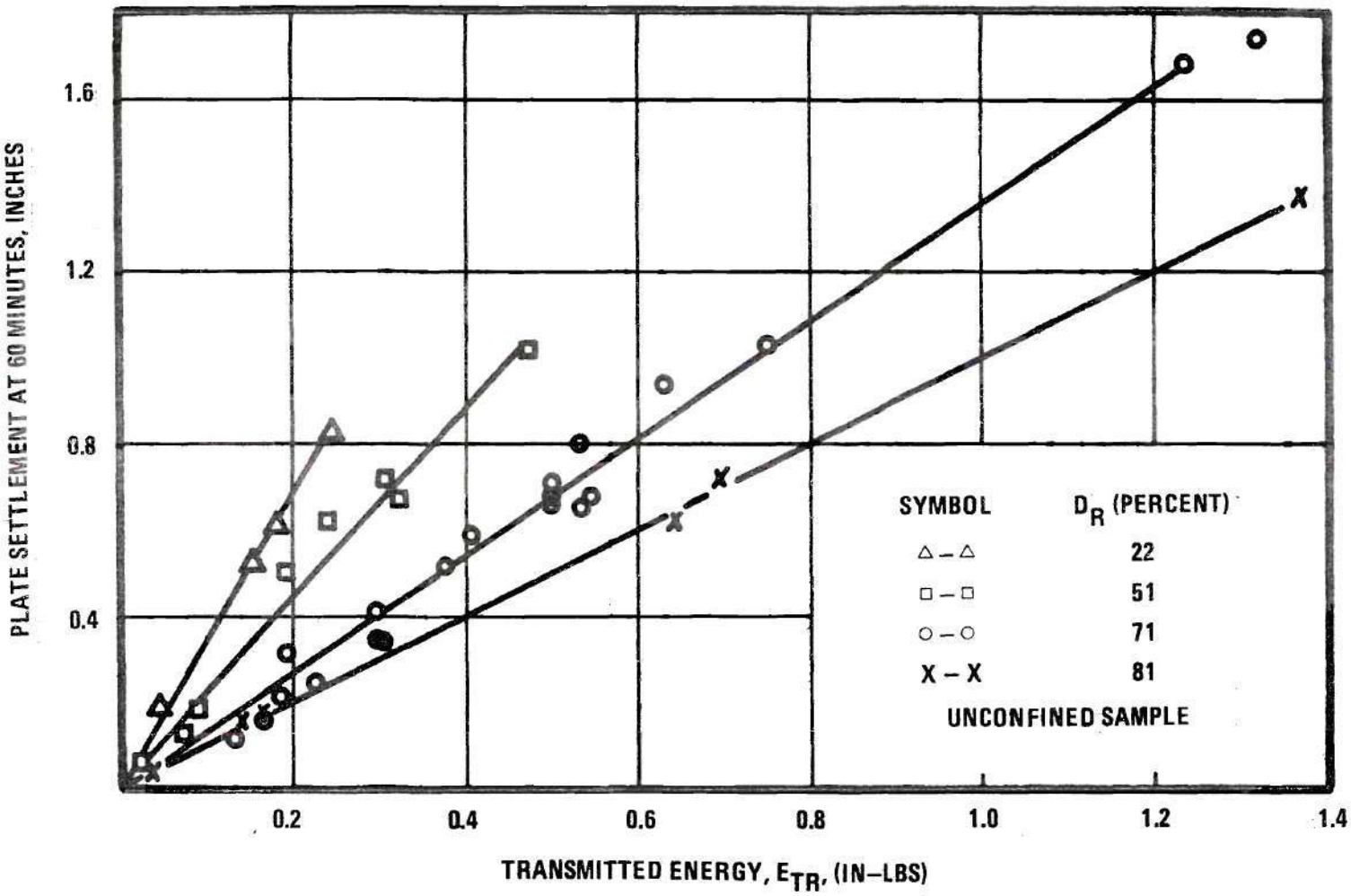

Figure 16. Steady–State Transmitted Energy Per Load Cycle vs Plate Settlement

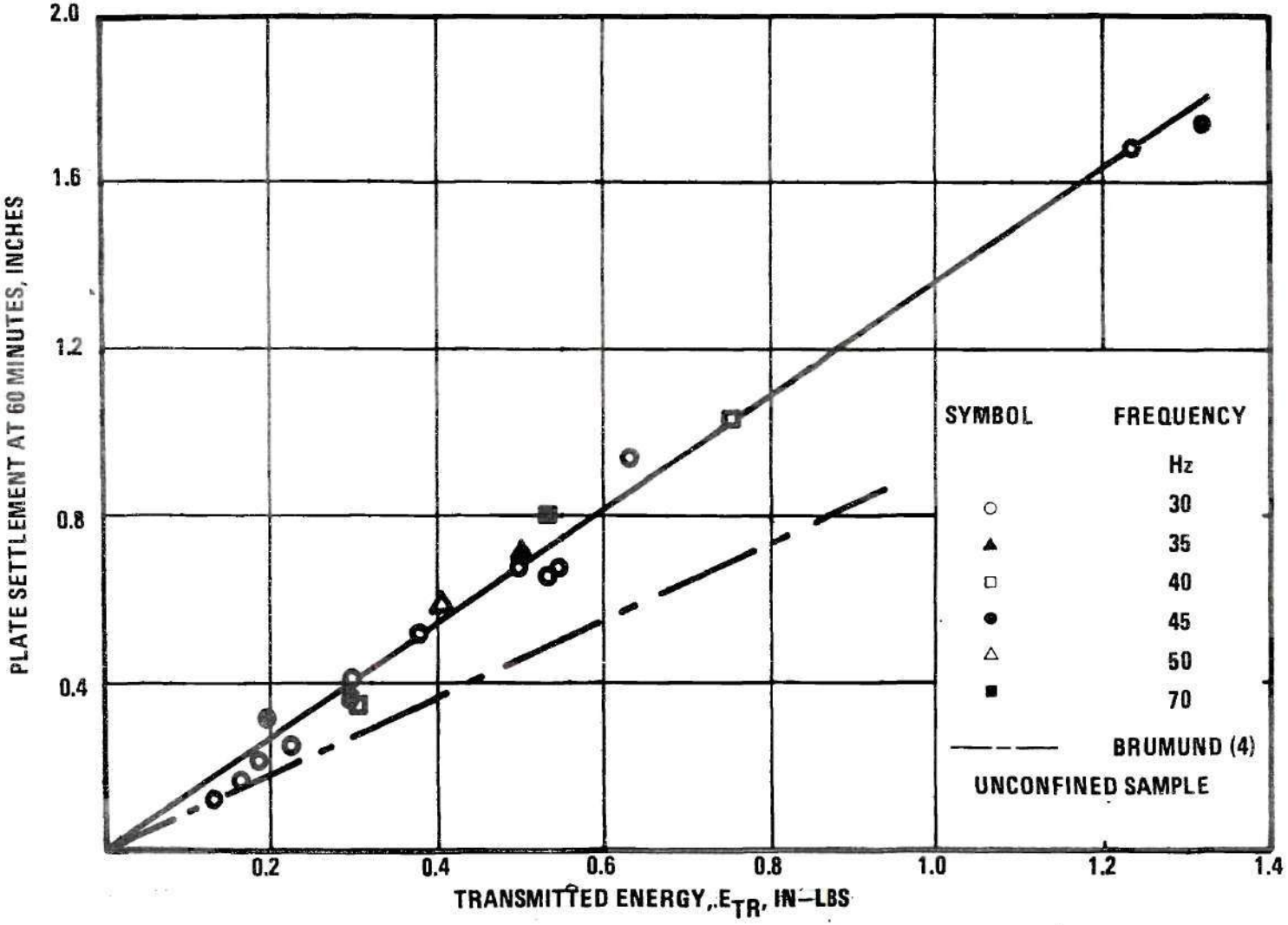

Figure 17. Steady–State Transmitted Energy Per Load Cycle vs Plate Settlement – D_R = 71 Percent

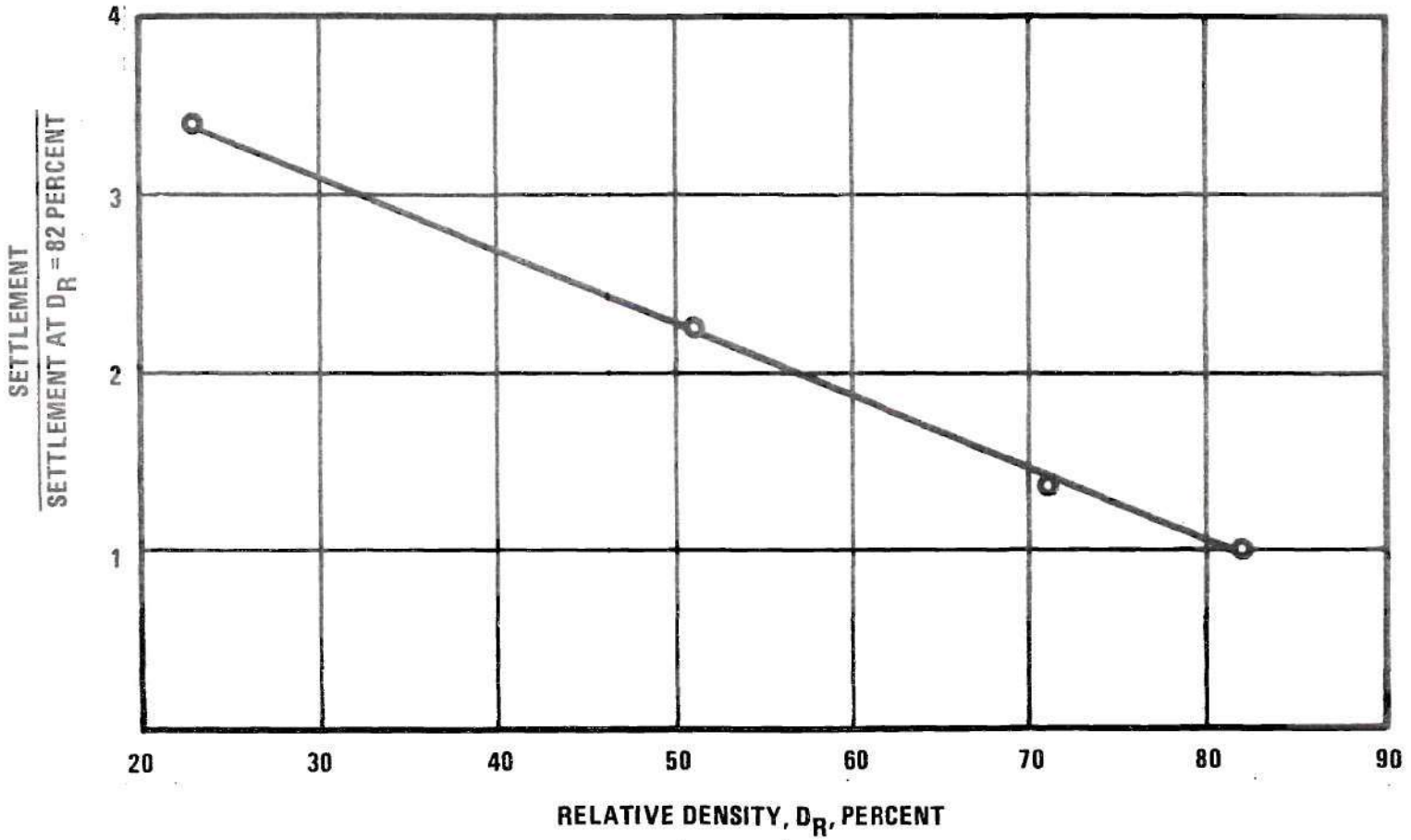

Figure 18. Normalized Settlement vs Relative Density for Unconfined Samples

Table 7. Results of Confined Sample Tests
With an Approximate Relative Density of 49 Percent

Test No.	D_R (%)	Freq. (Hz)	Static Load (lbs)	Dynamic Load (lbs)	A_p X 10^3 (inches)	E_{TR} (in-lbs)	H_o (inches)	S_{60}/H_o X 10^3
27c	50.0	30	200	120	2.43	0.486	5.954	13.320
28c	48.9	30	200	80	1.55	0.310	5.970	8.282
29c	50.0	30	200	40	1.09	0.218	5.962	4.613
30c	48.9	30	200	20	0.36	0.108	5.962	1.817

Table 8. Results of Confined Sample Tests
With an Approximate Relative Density of 70 Percent

Test No.	D_R (%)	Freq. (Hz)	Static Load (lbs)	Dynamic Load (lbs)	A_p X 10^3 (inches)	E_{TR} (in-lbs)	H_o (inches)	S_{60}/H_o X 10^3
2c	70.6	30	200	100	1.80	0.360	5.989	5.030
3c	72.0	30	100	50	1.10	0.110	6.010	2.870
7c	72.4	30	150	80	1.55	0.233	6.006	4.301
9c	71.6	30	110	20	0.50	0.055	5.990	2.180
10c	72.0	30	150	60	1.33	0.200	5.996	4.054
12c	72.4	30	250	180	3.43	0.858	5.961	7.222
26c	70.6	30	250	150	2.74	0.685	5.968	6.609

Table 9. Results of Confined Sample Tests
With an Approximate Relative Density of 82 Percent

Test No.	D_R (%)	Freq. (Hz)	Static Load (lbs)	Dynamic Load (lbs)	A_p X 10^3 (inches)	E_{TR} (in-lbs)	H_o (inches)	S_{60}/H_o X 10^3
18c	81.8	30	300	100	1.66	0.498	5.978	3.902
19c	81.8	30	300	50	0.96	0.288	5.968	3.025
22c	83.6	30	300	5	0.19	0.057	5.979	0.418
23c	83.6	30	300	20	0.43	0.129	5.981	1.299
24c	82.8	30	300	180	3.54	1.062	5.989	6.669
25c	82.8	30	300	150	2.61	0.783	5.960	5.406

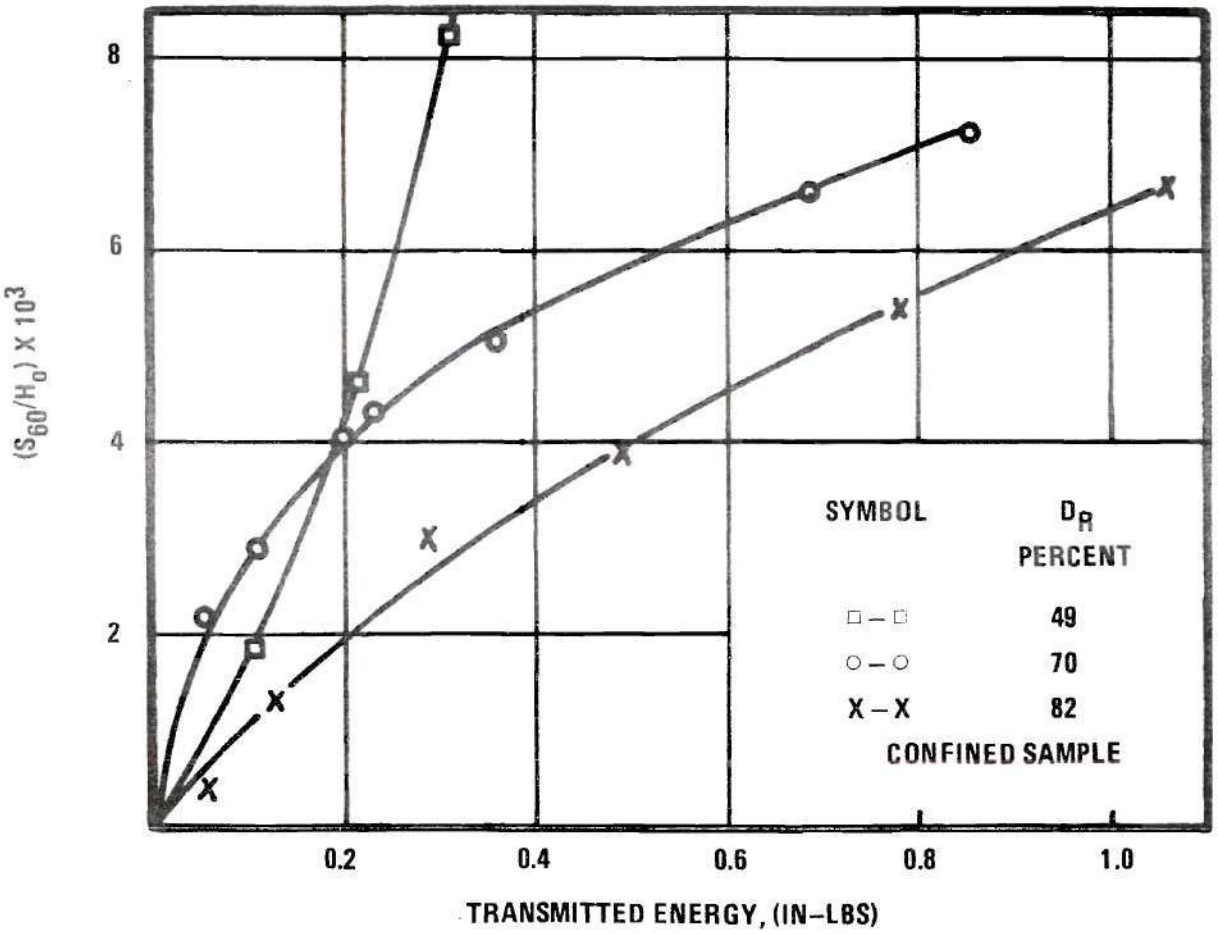

Figure 19. Steady–State Transmitted Energy Per Load Cycle vs Normalized Plate Settlement For Confined Samples

49, 70, and 82 percent. The relationships between normalized settlement and the logarithm of steady-state transmitted energy per load cycle are shown in Figure 20.

Dynamic Force-Amplitude of Vibration Relationship

Figure 21 reveals that there is a linear relationship between amplitude of vibration after 60 minutes of loading and applied dynamic force. This figure also indicates that for any given static weight there is a unique linear relationship. The density of the sand also affects this relationship as Figure 22 shows.

Frequency Response of Soil-Vibrating Plate System

The response of the soil-vibrating plate system was observed for frequencies of 30, 40, 45, 50, 60, and 70 Hz. The steady-state (after 60 minutes of loading) frequency response of the soil-vibrating plate system with respect to the amplitude of vibration of the plate divided by the dynamic force (similar to magnification factor) is indicated in Figure 23.

Soil Strain Gage Movement

The movement at different depths within the unconfined sand mass due to surface vibrational loading was determined using inductance type coil soil strain gages (see Appendix B for a description of these gages).

Figure 24 indicates the strain or change in gage

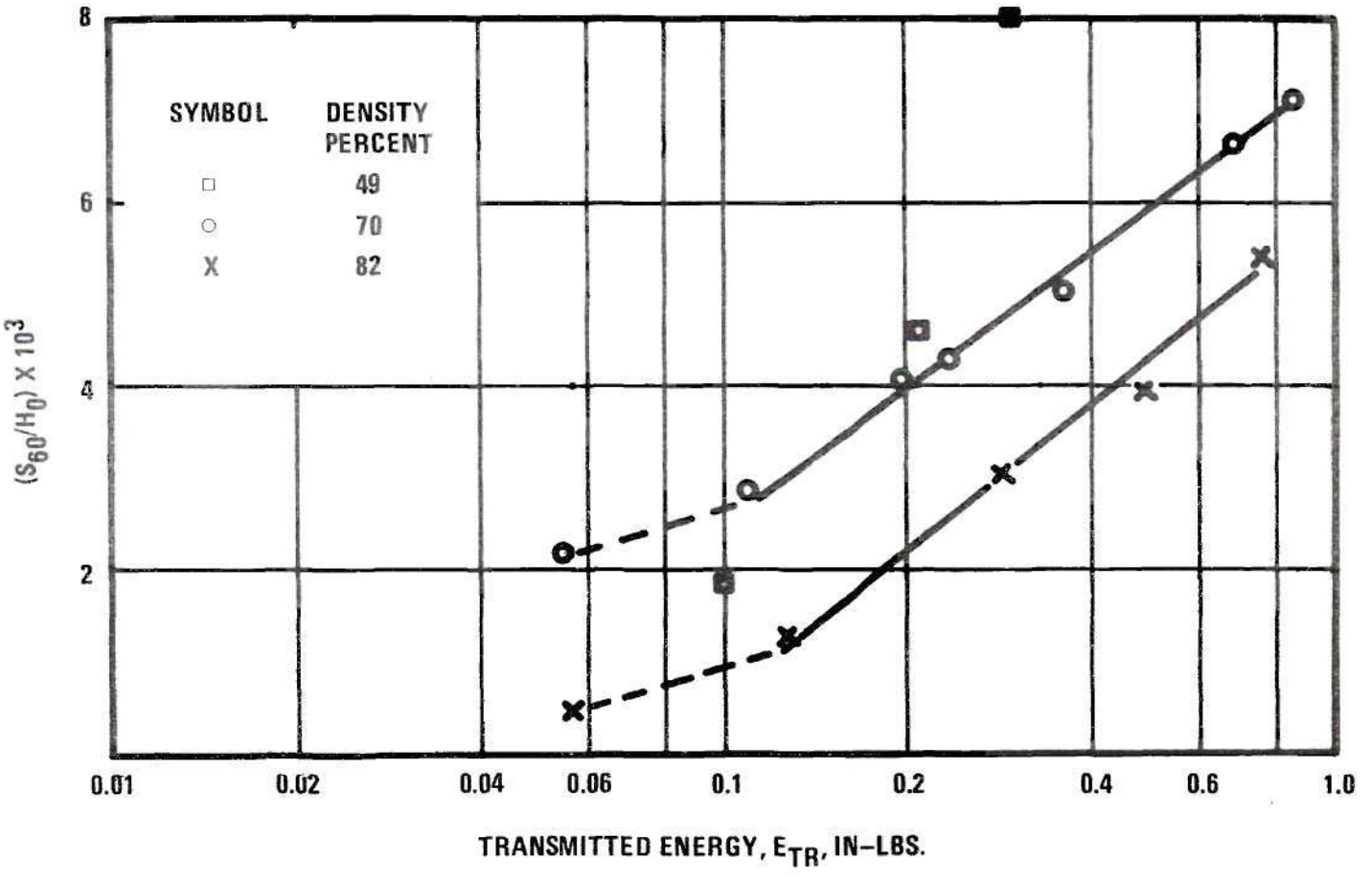

Figure 20. Normalized Settlement vs Logarithm of Steady-State Transmitted Energy Per Load Cycle For Confined Samples

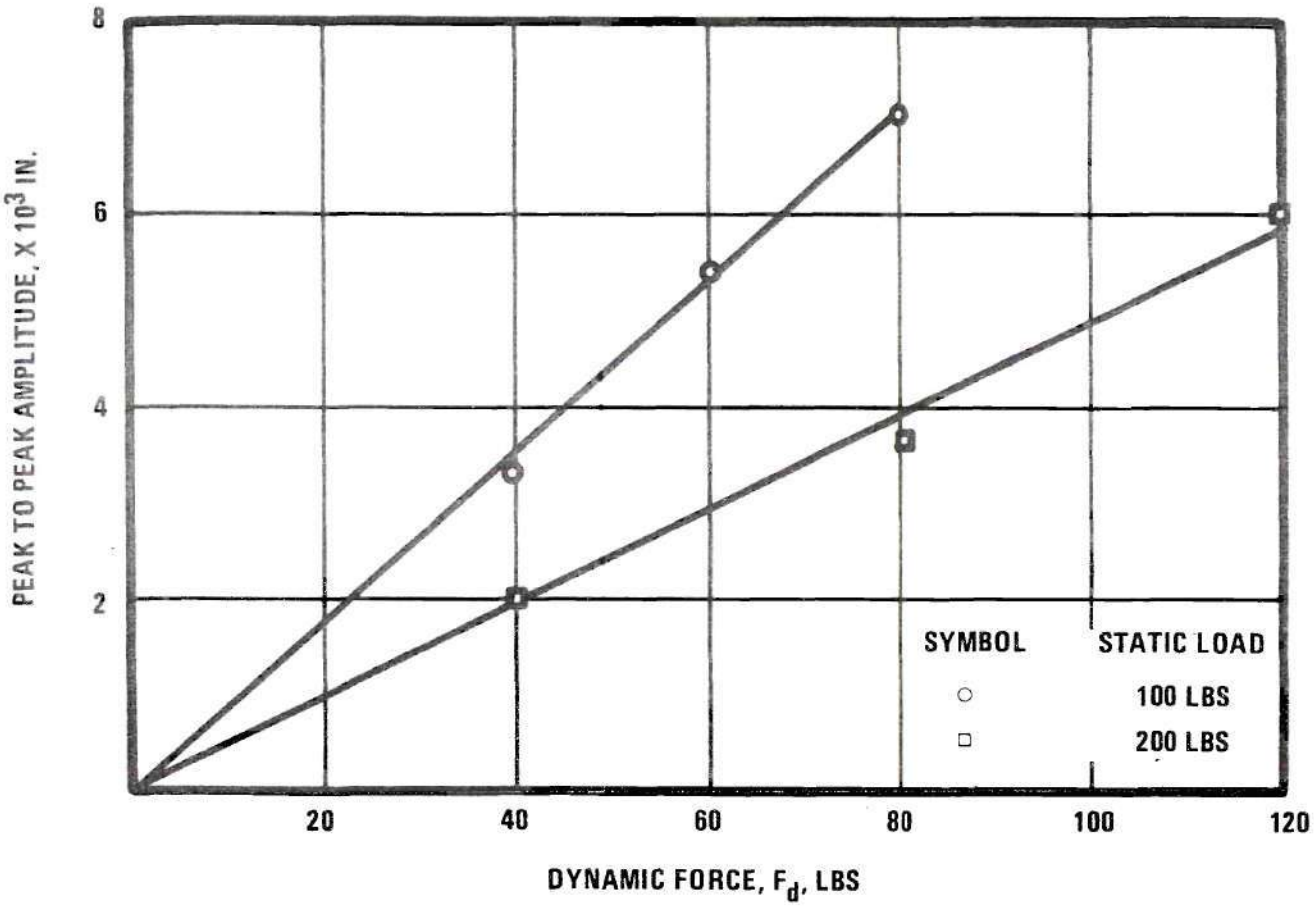

Figure 21. Steady–State Dynamic Force vs Peak-to-Peak Amplitude for Frequency = 30 Hz and D_R = 71 Percent

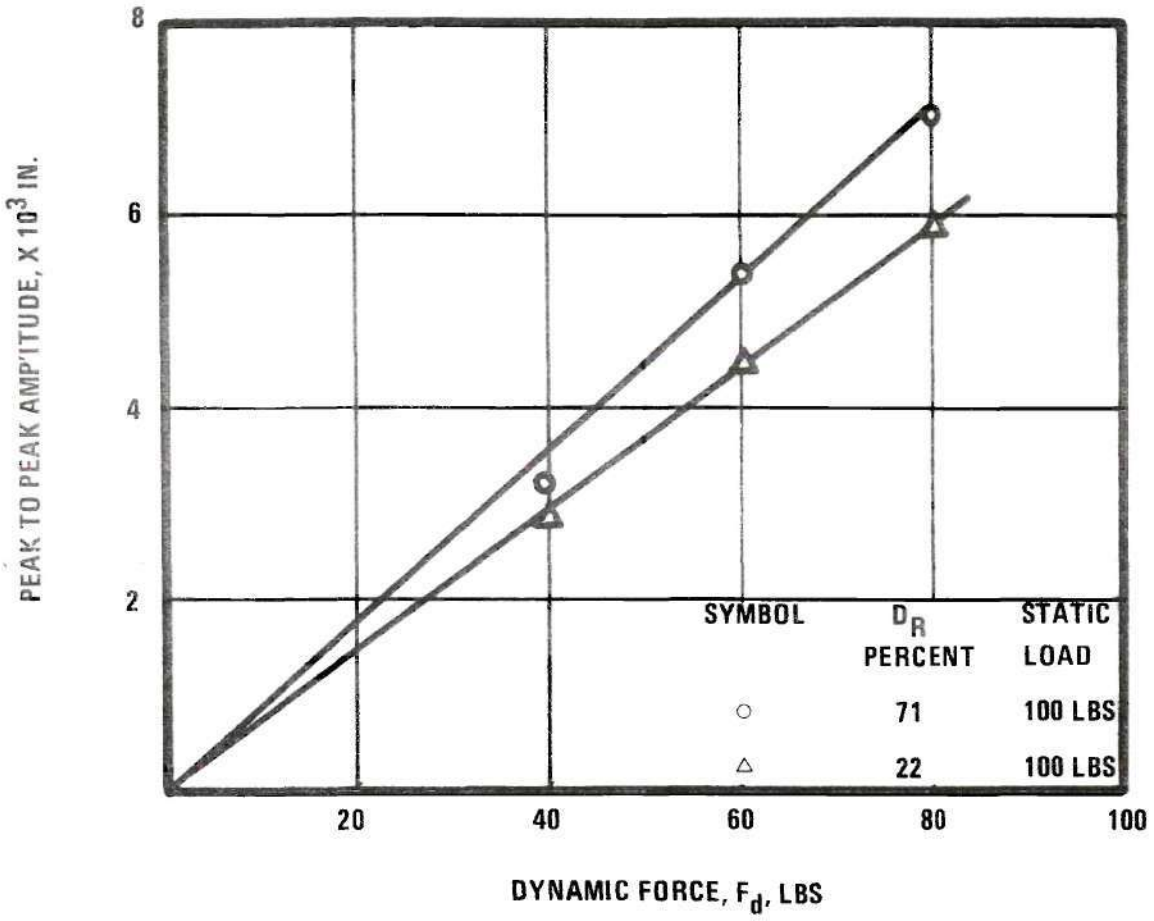

Figure 22. Steady–State Dynamic Force vs Peak-to-Peak Amplitude for Frequency = 30 Hz

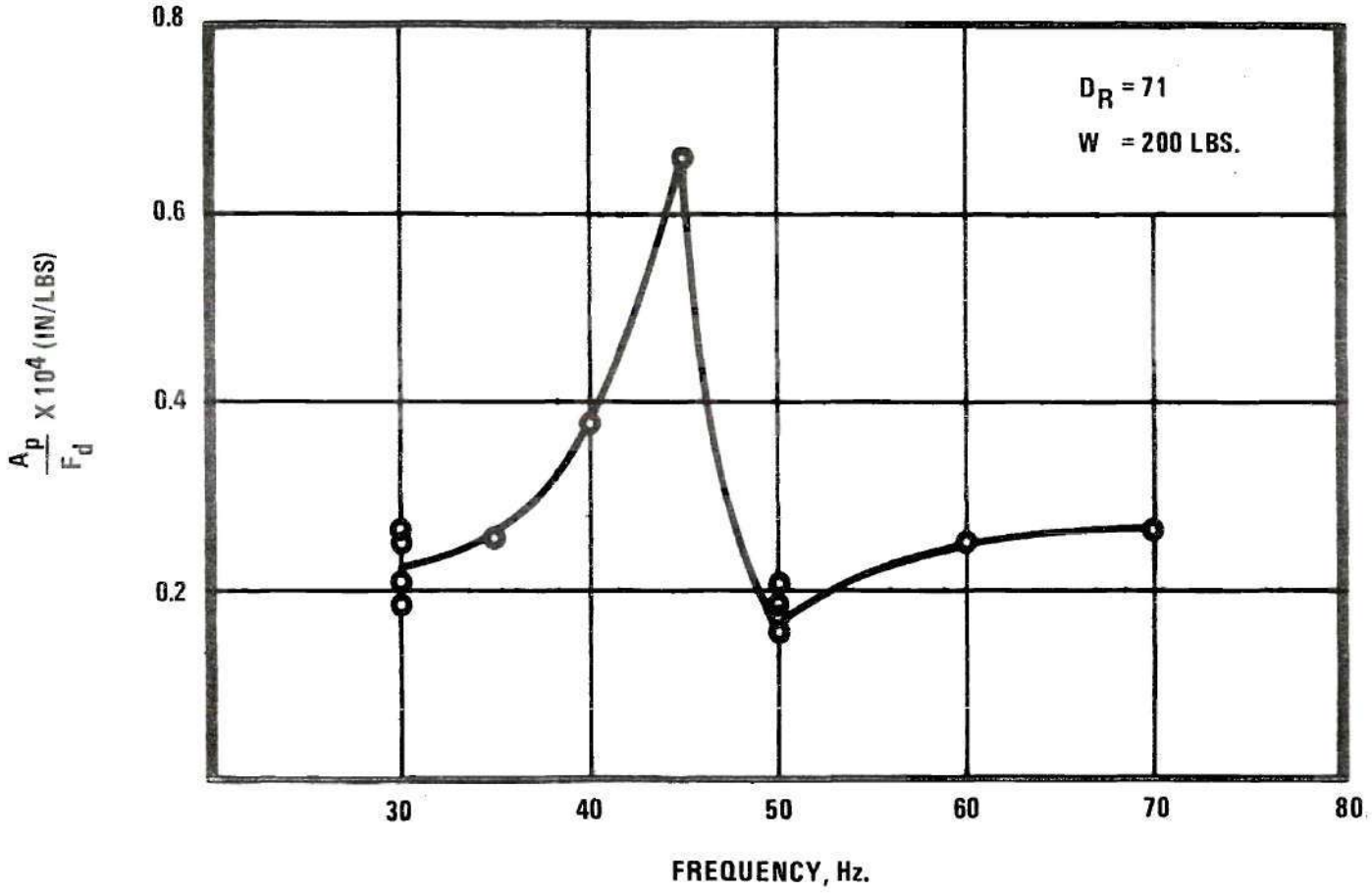

Figure 23. Frequency Response of Soil-Vibrating Plate System

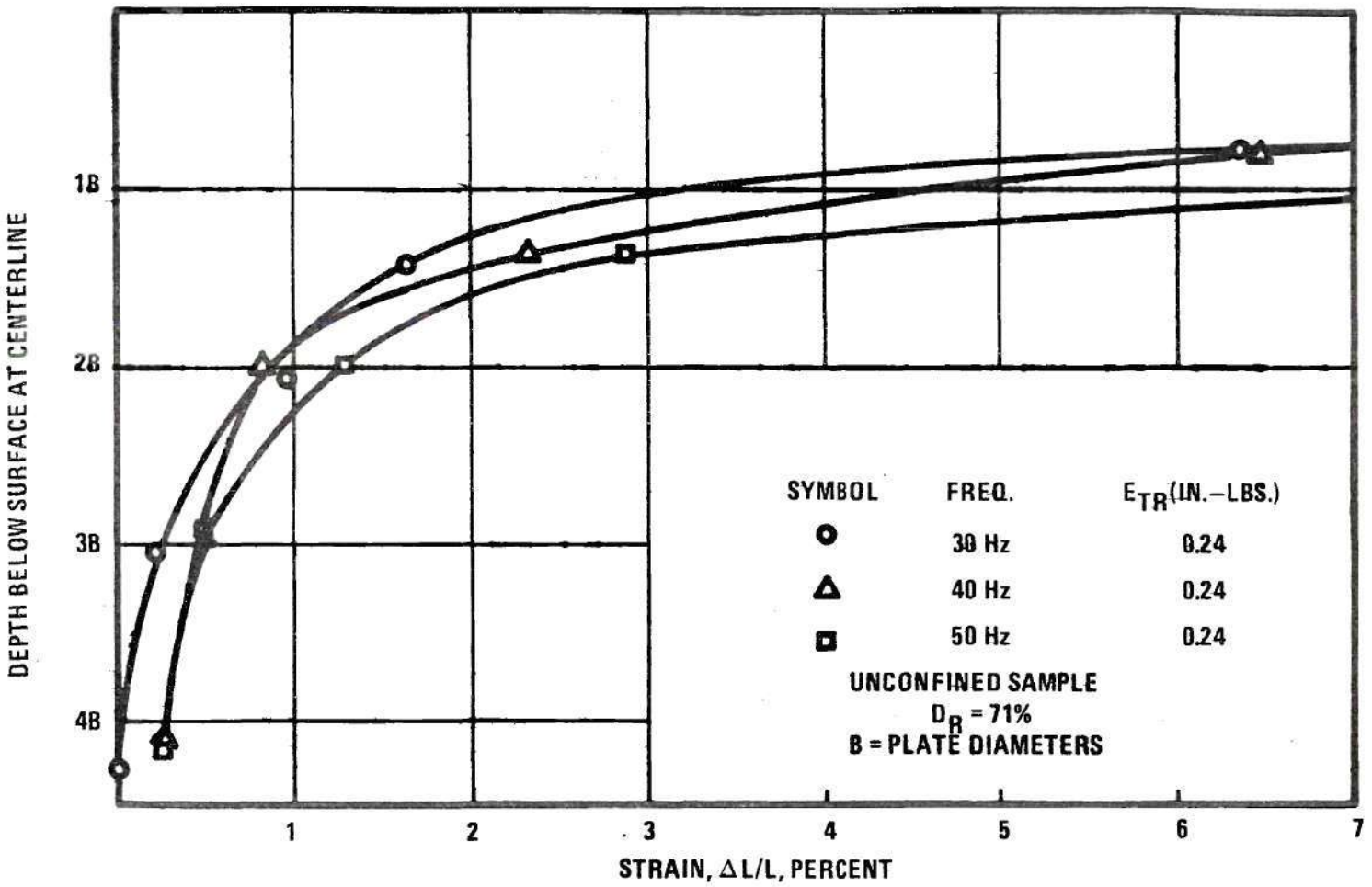

Figure 24. Soil Strain Gage Strain vs Depth of Embedment for Various Frequencies of Vibration.

separation with respect to original gage separation between gages caused by approximately equal steady-state transmitted energy per cycle at different vibrational frequencies. This figure shows the results of tests performed at frequencies of 30, 40, and 50 Hz. A comparison of the strain between gages caused by tests having different transmitted energies but frequencies of 40 Hz. is shown in Figure 25.

Figure 26 indicates the normalized movement (change in gage depth divided by the plate settlement at 60 minutes) of the soil strain gages with respect to the original gage depth. These curves are for the same tests as described above for Figure 24.

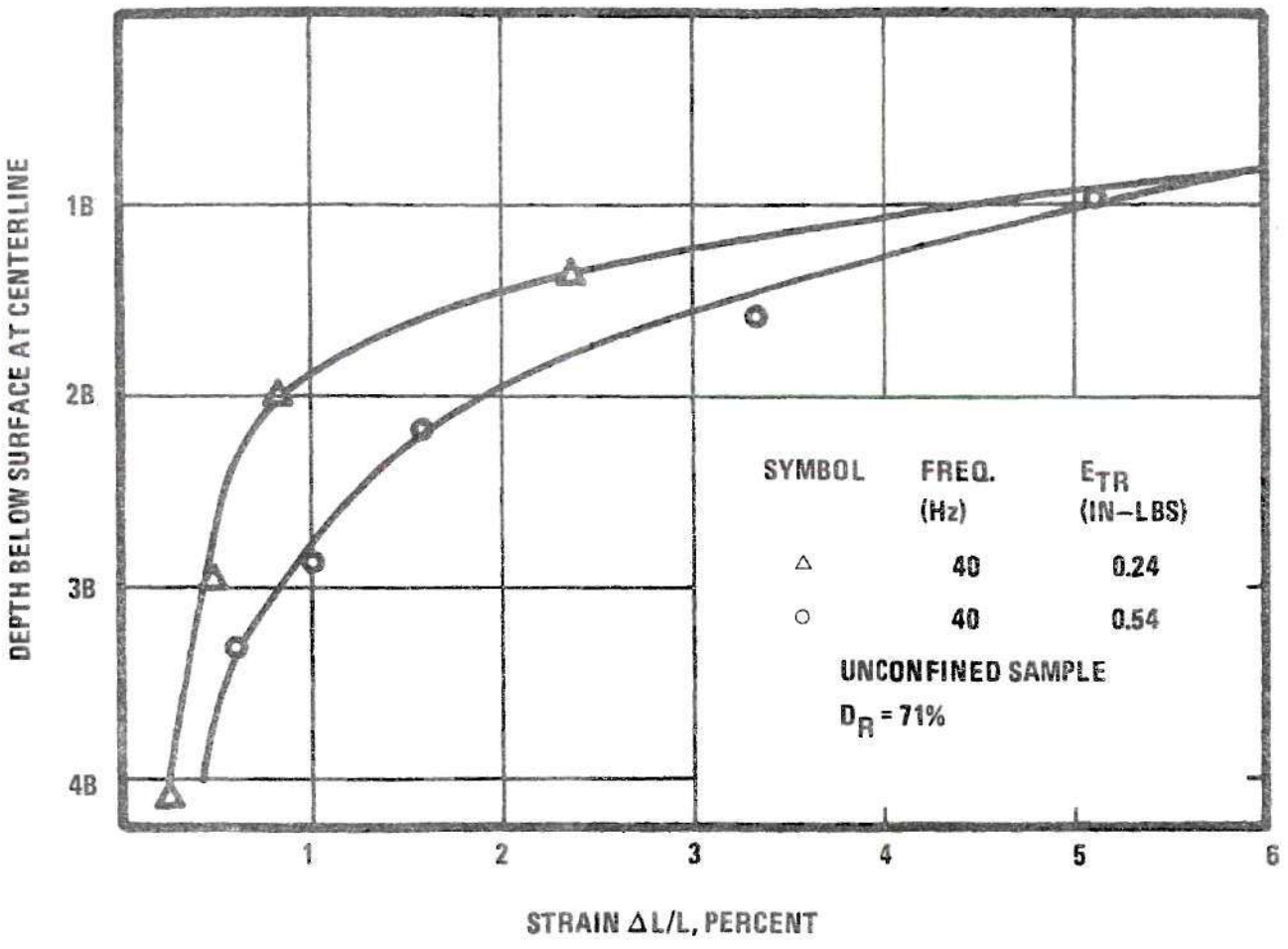

Figure 25. Soil Strain Gage Strain vs Depth of Embedment for Different E_{TR}

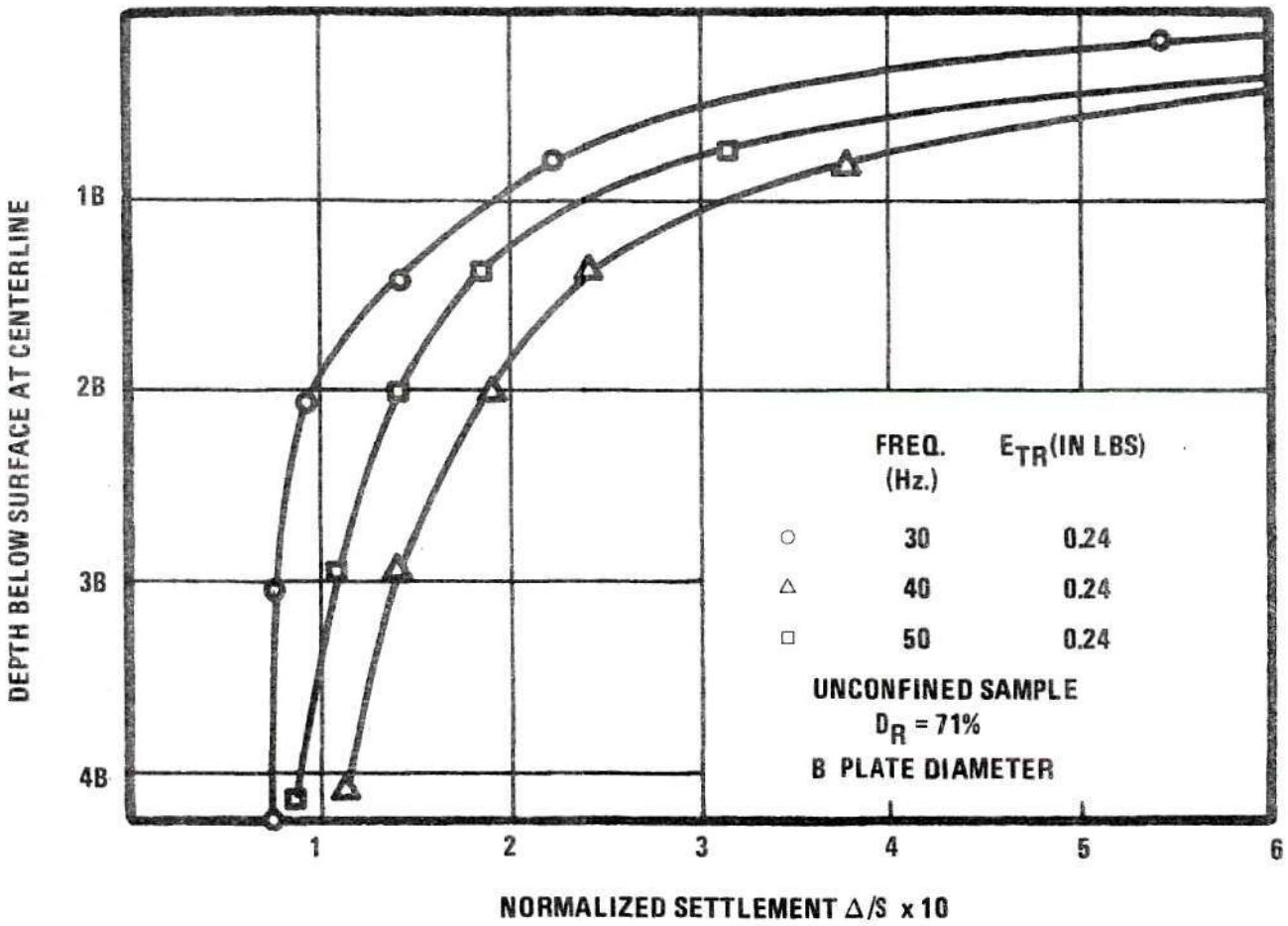

Figure 26. Soil Strain Gage Normalized Movement vs Depth of Embedment

CHAPTER XI

DISCUSSION OF RESULTS

Static Load Tests

A static load test was performed at each relative density used in the dynamic testing program to aid in the selection of allowable combinations of static and dynamic loadings. In most cases, the load combination totals (static load plus maximum downward dynamic load) were chosen such that the static load beyond which there was a significant increase in the settlement due to an increase in static load was 30 percent greater than maximum applied loads.

Test Duration

After studying the time-settlement results of other researchers and conducting some preliminary tests, the time of 60 minutes for the duration of the tests was chosen.

Prakash and Gupta (30) arrived at a steady-state settlement condition after vibrating their shaker table for approximately 20 minutes, while Brumund (4) required 60 minutes of vertical plate vibrations before approaching a steady-state settlement condition. Tanimoto (40) using vertical plate vibrations approached a steady-state

settlement condition after 10 to 15 minutes. Since there seemed to be a wide variance in time necessary to reach a near steady-state condition, tests were run using the 60 minute criteria. As Figure 13 indicates, the time-settlement curves are approaching a steady-state condition at 60 minutes of test duration. Therefore, since the general shapes of the time-settlement curves in Figure 13 are analogous to those obtained by the researchers mentioned above, the 60 minute time duration was selected. Also, since the objective of these tests was to verify and develop concepts governing vibratory compaction and not to arrive at precise quantitative values for ultimate settlement, the 60 minute test was adequate for the needs of this project.

Figure 14 and Figure 15 indicate for the unconfined and confined samples that on a semi-logarithmic plot the rate of increase in settlement was linear through approximately four minutes of dynamic loading time or 7,200 cycles for a 30 Hz. frequency of vibration. Beyond four minutes the curves ceased to be linear. Converse (7), loading unconfined samples, found that settlement was linear with respect to the logarithm of time for 6,000 cycles of loading. Brumund (4), also loading unconfined samples, determined that settlement was linear with respect to the logarithm of time for cycles of loading up to 18,000; beyond 18,000 cycles the relationship was not linear. D'Appolonia

(10, 11), however, determined that the linear relation between the logarithm of time of load application and settlement was valid for load applications of 10^5 cycles. His work, however, was performed using frequencies of 6 Hz. or less. Therefore, at low frequencies, less than 10 Hz., or for cycles of loading less than 7,000 to 18,000 settlement is a linear function of the logarithm of time.

Effects of Test Bin Vibration Wave Reflection on Unconfined Tests

To further insure the validity of the results and eliminate the possibility of test artifacts, tests were performed to determine the wall reflective characteristics of the test bin. Tests were performed to determine if the concrete block walls of the test bin produced too much energy reflection; this was accomplished by performing replicate tests with the bin lined with a polyurethane foam, similar to that which Ho and Burwash (17) used.

As Table 1 indicates, there was a significant effect on the settlement of the vibrating plate due to the wall reflectance. With the walls of the test bin lined with polyurethane foam, the settlements were at least 15 percent less for a 30 Hz. frequency of plate vibration than those tests performed with unlined test bin walls. The difference was definitely dependent on the frequency of plate vibration as Table 1 indicates. For frequencies of 40 Hz.

and 50 Hz. the reductions in settlement were approximately 35 and 50 percents.

The foam material was a sufficiently low elastic (very low combination of modulus of elasticity and moment of inertia) material to absorb the energy of any vibrational waves transmitted through the sand mass to the walls. Therefore, there was little or no vibration wave energy reflected from the wall back to the sand. The concrete block walls, however, had a much larger combination of modulus of elasticity and moment of inertia in comparison to the foam, and this caused the reflection of the energy transmitted by any vibration waves through the sand to the wall. Therefore, the sand mass was being subjected to the energies of the original vibrational waves and those reflected from the rigid test bin walls. This cumulative effect caused the increase in settlement of the vibrating plate for these tests over tests performed with the sides lined with foam. Therefore, all final results were generated with the test bin lined with one inch thick polyurethane foam.

Plate Settlement-Transmitted Energy Relationship

Figure 16 shows the relationships between settlement of the five inch plate and transmitted energy for four different relative densities of the unconfined sand mass. As the data in this Figure 16 indicate, the settlement of the plate was a linear function of the steady-state

transmitted energy per load cycle. For each density, a least square linear regression analysis was used to develop the relationship. The energy-settlement data obtained when the soil strain gages were in the sand mass are not shown in Figure 16. The inclusion of the gages seemed to affect the energy-settlement relationship slightly. The gage inclusion tended to cause some of the settlements to be larger than predicted by Figure 16, probably because of wave reflection off the smooth, hard gage faces.

There are several facts that Figure 16 reveals. First, the linear relationship between settlement and steady-state transmitted energy per cycle of load application, as first proposed by Brumund (4), was valid using a much different type of sand. Brumund used a uniform Ottawa sand which had rounded quartz particles, while the sand used in this study, as described earlier, had angular quartz and mica particles. As Figure 17 and Table 10 indicate, the results of this study produced a slope (settlement/steady-state transmitted energy) of 1.35 for a relative density of 71 percent, while Brumund in his study using a four inch diameter plate obtained a slope of 0.91 for a relative density of 70 percent. The initial void ratios for the two sands were significantly different, and this difference may partially explain the differences in slopes. The type and gradation of sand used in each study also

Table 10. Comparison of Results With Those Obtained by Brumund (4)

	D_R (%)	C_u	γ (lbs/ft^3)	e	M* in/(in-lbs)
Skelton	71	2.53	99	0.66	1.35
Brumund (4)	70	1	107	0.54	0.91

* M = settlement at 60 minutes/steady-state transmitted energy

contributed to the slope difference. The difference in the size of plates used also contributed to the difference in slopes. The larger the plate size, the larger would be the slope, which would when comparing two sands tend to increase the differences in slopes. Thus, the proposed linear relationship between settlement and steady-state transmitted energy is valid for each type of sand. Each sand will have its own unique relationship between settlement and steady-state transmitted energy.

The second fact that Figure 16 reveals is that settlement was proportional to transmitted energy for essentially any relative density that a sand may attain. This point, although suggested by Brumund, had not been proven by experimental or theoretical evidence. Figure 18, showing the sensitivity of settlement to relative density, further illustrates this position. This figure indicates

that the ratio of settlement at any density to settlement at a relative density of 82 percent was a linear function of relative density. Thus, the relative structure (low relative density, 22 percent, implying that the sand is in a collapse condition) of the sand mass does not affect the proposed relationship. The ratios of settlements shown in Figure 18 may be partially quantitatively explained by examining the possible change in void volume possible at each relative density. Table 11 indicates the initial available void volume for each relative density and the difference between the void volume at 82 percent relative density and the void volumes of the three remaining relative densities.

Table 11. Available Void Volume For Each Relative Density

D_R (%)	Initial V_v ft^3/ft^3	$V_v - V_{v82}$ ft^3/ft^3	$S_N^* - 1$	$\frac{(S_N - 1)_{51}^{82}}{V_{v51} - V_{v82}}(V_v - V_{v82})$
82	0.385	0	0	0
71	0.400	0.015	0.35	0.54
51	0.425	0.035	1.25	1.25
22	0.449	0.064	2.39	2.28

* S_N = settlement/(settlement at D_R = 82 percent)

The change in initial void volume between 82 percent and 51 percent relative density was 0.035 ft^3/ft^3. This difference in initial state resulted in more settlement for the same energy input as is shown in Figure 18. If the increase in settlement per increase in void volume for 82 percent and 51 percent relative density is extrapolated to other relative densities, as shown in Table 11, the extrapolation agrees reasonably well with observed settlements. Table 11 indicates that much of the increased settlement can be explained by examining the increased void volumes; however, Table 11 also indicates that a slightly greater proportion of the settlement is due to shear distortion at the lower relative density.

The majority of the transmitted energy data presented in Figure 16 is based on the use of the Equation 6 below.

$$E_{TR} = A_p \cdot F_{TR} \qquad (6)$$

As long as the phase shift angle between the contact force and the vibration amplitude was small, Equation 6 yielded a sufficiently accurate value for transmitted energy; however, if a significant phase shift is present (e.g. operation near resonance) then the transmitted energy must be determined more accurately. A phase shift represents an

energy loss per cycle of vibration and would appear as the area within a hysteresis loop formed by plotting contact force versus vibration amplitude. The true energy would be determined by intergating the area under the loading force-displacement function. Figures 27, 28, and 29 for frequencies of load applications of 30, 40, and 50 Hz. show the Lissajous figures for tests having a relative density of 71 percent, a static force of 100 pounds, and a different dynamic force for each frequency. These tests were representative of all the tests. As these figures indicate, the areas under the Lissajous (hysteresis) curves are not significantly larger than those predicted by Equation 6. The value of E_{TR} as determined from Equation 6 was found to be within 90 percent of the true transmitted energy. Therefore, the error in using Equation 6 was considered minimal.

The individual values of amplitude of vibration and average contact force were other sources of possible error in the calculated transmitted energy values. However, by measuring the amplitude of vibration of the loading plate with a linear variable differential transducer mounted so as to not be affected by external or spurious vibrations, movements of the plate only were measured. The values of average contact force were obtained from the output of the load cell located just above the loading plate. In this position, only the inertia effects of the loading plate and

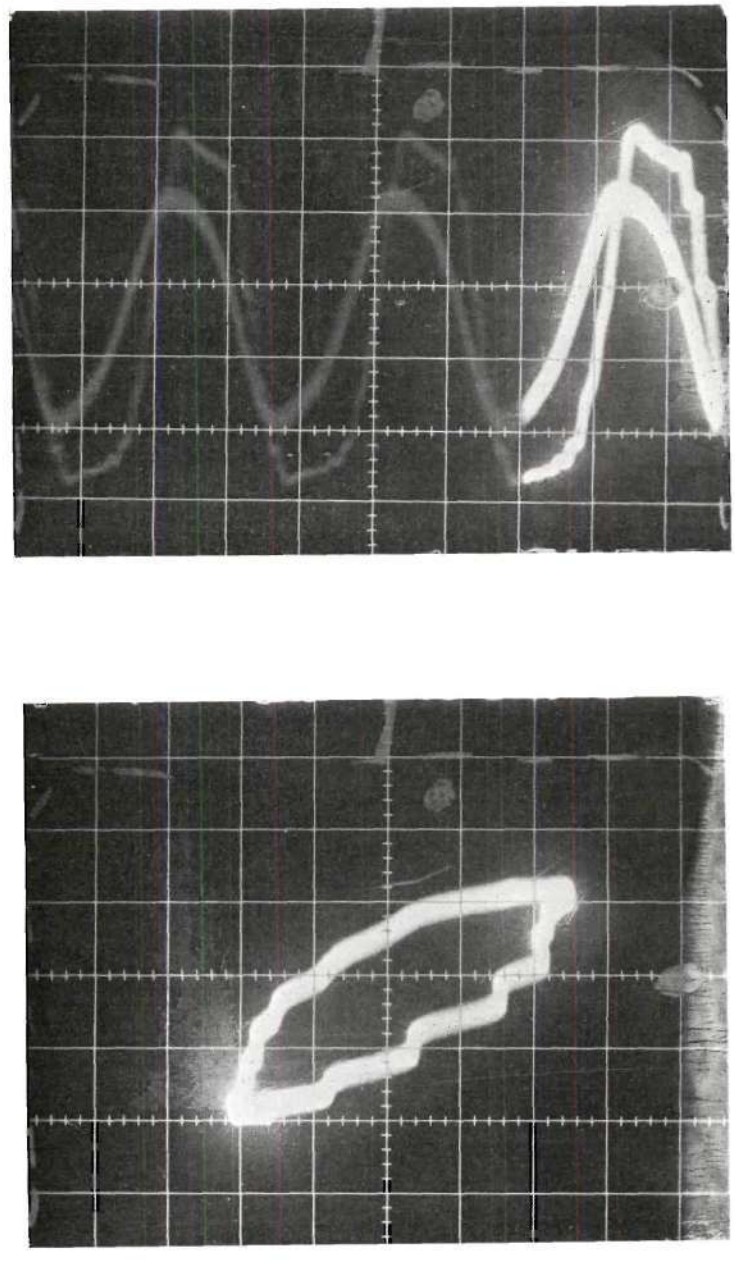

Figure 27. Steady-State Wave Form and Hysteresis Loop for 100 Pound Static Force and 30 Hz. Frequency

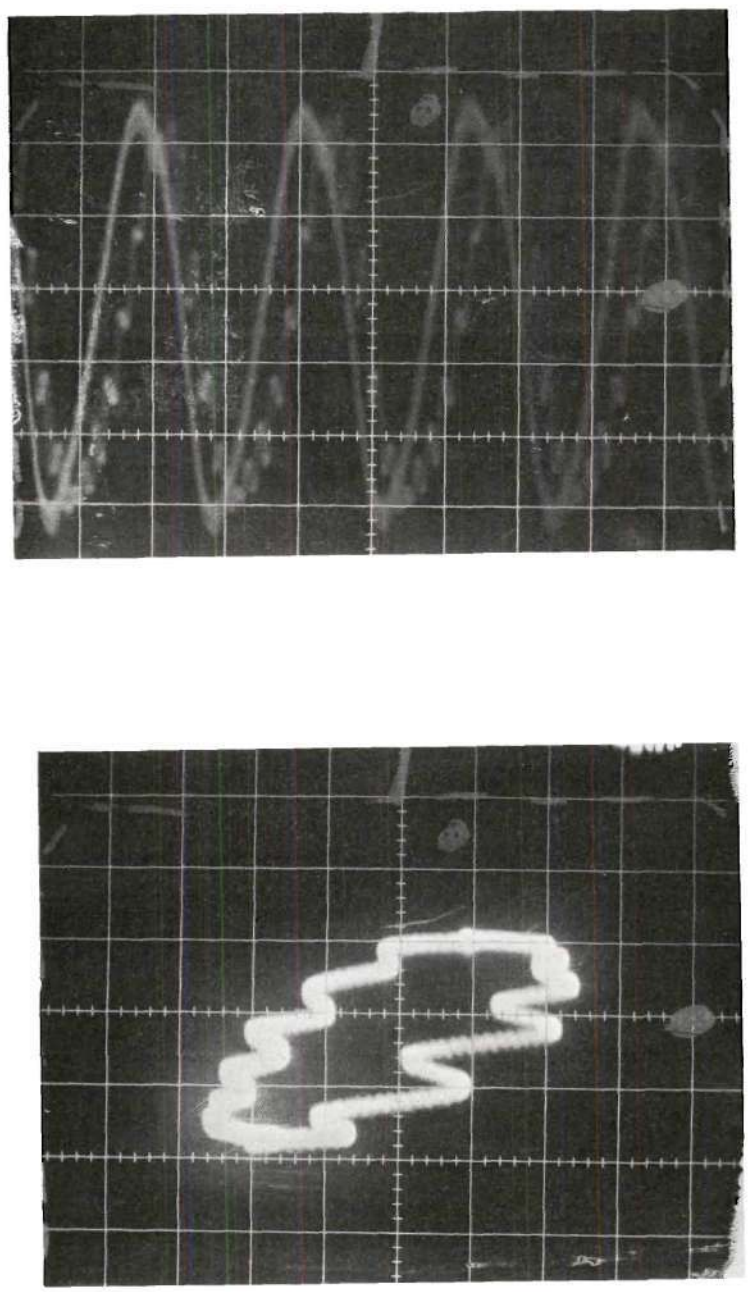

Figure 28. Steady-State Wave Form and Hysteresis Loop for 100 Pound Static Force and 40 Hz. Frequency

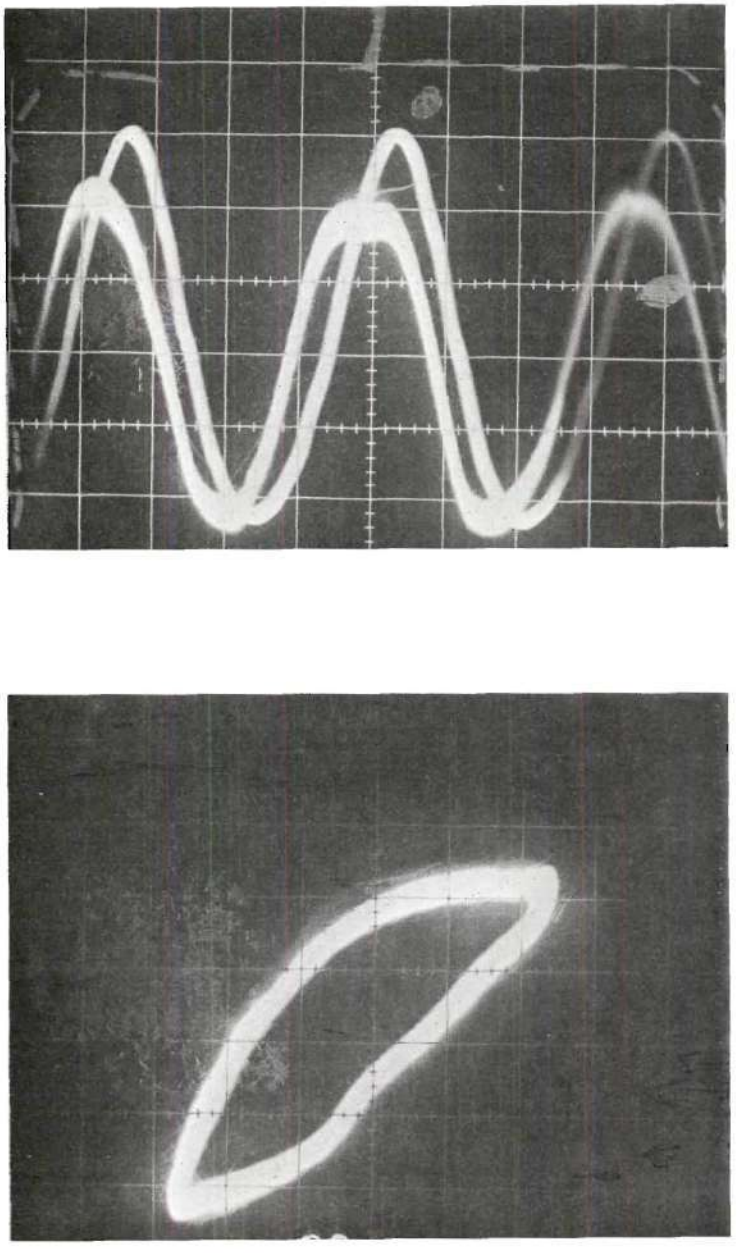

Figure 29. Steady-State Wave Form and Hysteresis Loop for 100 Pound Static Force and 50 Hz. Frequency

the adaptor could affect the output of the load cell. Tests were performed with the plate vibrating in the air with no material below it at the same vibrational amplitudes and frequencies as during tests on the sand mass. The maximum inertia loads measured by the load cell for these tests were less than one to two pounds. Consequently, inertial effects of the loading plate were considered negligible.

Confined Sample Tests

Tests were performed on confined samples to obtain a relationship between densification and surface settlement of a vibrating plate. The settlement of a vibrating plate can be due to two factors; settlement due to shear strain at constant volume and settlement due to volume decrease or densification.

In the confined sample tests the entire surface of the sample was loaded, and therefore the sand sample was confined against any lateral movement (shear distortion at constant volume). Therefore, any settlement of the vibrating plate was due entirely to the densification of the sand sample. Thus the shape of the curves of normalized settlement versus steady-state transmitted energy per load cycle shown in Figure 19 would be identical to the shape of densification versus transmitted energy. As this figure indicates, there is not a linear relationship between

densification or settlement on confined samples and transmitted energy per cycle of loading for the relative densities of 71 and 82 percents. Figure 20 shows densification to be a linear function of the logarithm of transmitted energy except at very small transmitted energy levels where there is some deviation due to frictional losses and errors in measurement. However, these small transmitted energy levels are below the normal range of interest. At a relative density of 50 percent, the densification was very large. The complete shape of the curve for this relative density was not determined. However, it is felt that no fundamental change in behavior occurs at this relative density. Therefore, the densification versus logarithm of transmitted energy relationship would probably be linear if a wider range of transmitted energies were tested at this relative density.

It was very difficult to compare quantitatively the confined and unconfined tests because of the different stress states in the samples. Densification and shear strain are very dependent on the confining stress; the confining stress changes in confined tests.

Dynamic Force-Amplitude of Vibration Relationship

Brumund (4) found that the amplitude of vibration was a linear function of the dynamic force for a constant static weight and frequency of plate vibration. Figure 21

verifies this result for the sand used in this study. This linear relationship was also found to hold true for each of the various densities of this test program.

Frequency Response of Soil-Vibrating Plate System

The amplitude of vibration per unit dynamic force response of the soil-vibrating plate system to frequency is shown in Figure 23 for a static weight of 200 pounds. The value of amplitude per unit dynamic force is essentially a magnification factor. The general shape of the response curve is the most important feature of Figure 23. This curve indicates that a resonant frequency of approximately 45 Hz. existed for a static weight of 200 pounds. This load corresponds to a pressure of 1,467 pounds per square foot on a five inch diameter plate. Eastwood (12), in his study of the resonant frequencies of circular footings, determined the natural frequencies of ten inch, eight inch, and six inch diameter plates for various static pressures. Figure 30 presents Eastwood's results. His results were extrapolated to estimate the predicted natural frequency for a five inch diameter plate subjected to a static pressure of 1,467 pounds per square foot. From this extrapolation, a predicted resonant frequency of approximately 46 Hz. was determined. This compared favorable to that shown in Figure 23.

Other researchers, Ho and Burwash (17) and Brumund

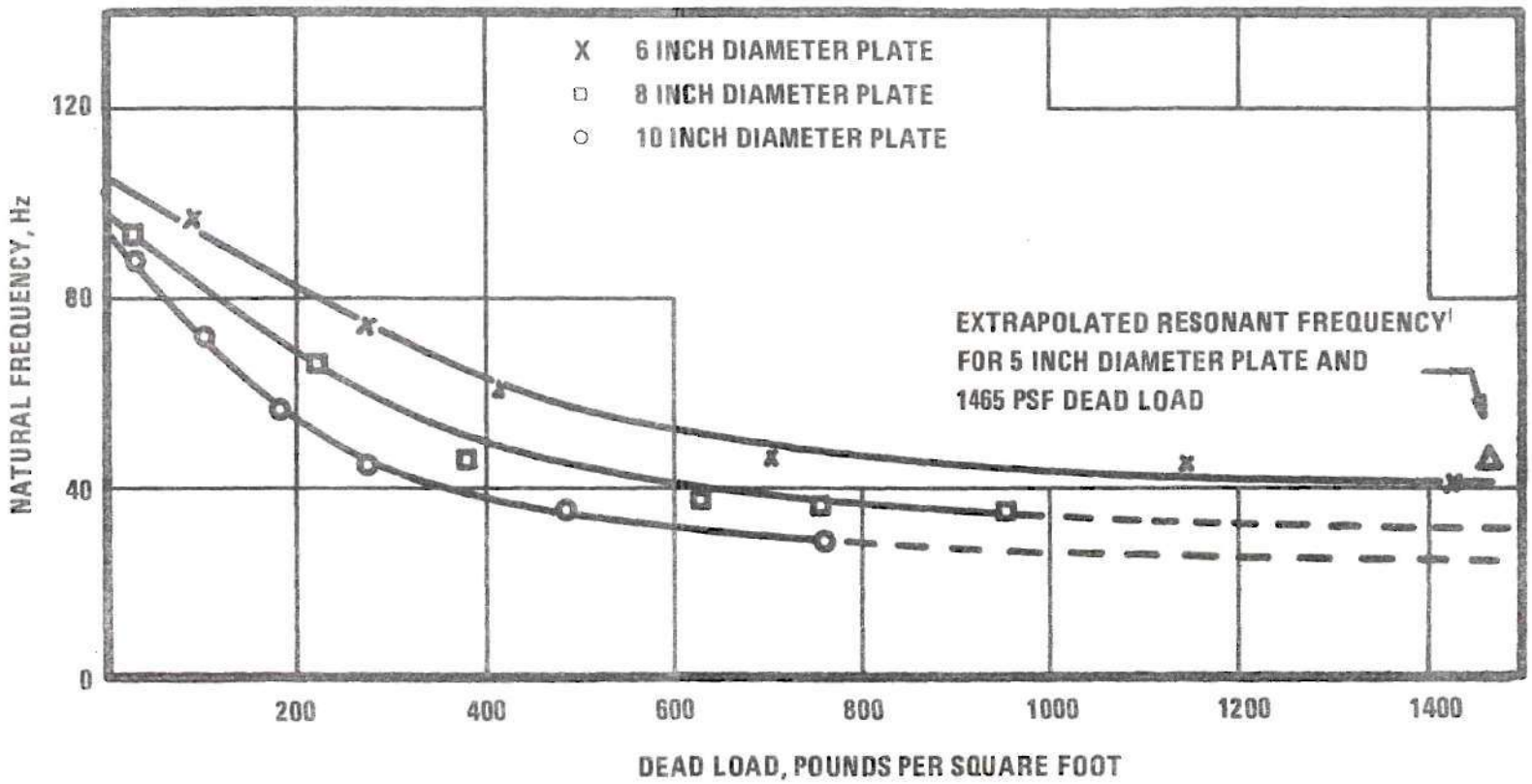

Figure 30. Natural Frequencies of Circular Footings on Dry Sand, After Eastwood (12)

(4), using vibrating plates of comparable size to those used by Eastwood observed resonant frequencies of 83 Hz. for static stress of 248 psf and 50 Hz. for static stress of 1120 psf. By extrapolating Eastwood's data, the predicted resonant frequencies were 79 Hz. and 52 Hz. Therefore, the results of Eastwood indicated a reasonably accurate prediction of the resonant frequency of vibrating circular plates acting on dry cohesionless materials.

The values of A_p/F_d at any given frequency were observed to have a slight dependence on the dynamic force, F_d.

Soil Strain Gage Movement

Although the results of the strain gage tests are not shown in Figure 16, as mentioned previously, they do provide some insight as to the relative zone of influence of surface vibration. The effects of frequency of plate vibration at approximately equal steady-state transmitted energies per cycle of load application on movements within the sand mass are shown in Figures 24 and 26. In Figure 24, the incremental strain, change in spacing divided by original spacing is shown, while Figure 26 presents the normalized movement (change in gage depth/plate settlement at 60 minutes).

Figure 26 indicates that below a depth B below the footing the axial strain is less than five percent for the

energies used; below 2B the axial strain is less than one percent. Figures 24, 25, and 26 are not meant to show depth to which compaction is occurring; this has been done adequately in the literature by D'Appolonia, Whitman and D'Appolonia (9) and Converse (7).

Figure 25 show how a difference in transmitted energy affects the movements within the sand mass. As this figure indicates, the higher the transmitted energy, the larger are the movements. The higher transmitted energy caused the depth of at least one percent strain (movement) to be at nearly three diameters compared to approximately two diameters for the lower transmitted energy. However, 95 percent of the strain still occurs within a depth of between one and two diameters for the higher transmitted energy level. Thus, the significant depth of movement and, therefore, densification and/or shear distortion occurs within one to two diameters below the surface.

Figures 24, 25, and 26 indicate the relative zone of influence due to surface vibration, and more importantly, how this zone changes with frequency (i.e., how does the zone of influence change when the vibrator operates near resonance). Within the limits of accuracy of the gages there appears to be no significant frequency effect on the zone of influence. This may contradict some of the statements by other investigators; Lewis (21), Johnson and

Sallberg (18), Forssblad (13), D'Appolonia, Whitman, and D'Appolonia (9), and Broms and Forssblad (3) have all stated that the most efficient use of a compactor is attained using operating frequencies of compactor vibration at or above the resonant frequency. (However, the term efficient is usually not defined.)

Selig (36) evaluated the effectiveness of using soil strain gages of the type used in this study to measure strains within a soil mass subjected to vibratory compactive efforts. Selig arrived at several conclusions concerning the gages. For coaxial (vertical axial alignment) configurations, offset and rotational misalignments were found to cause only slight inaccuracies in measurements. Independent direct measurements of gage spacings proved the electrically determined distances to be very accurate. This study confirms the reliability of using this type of electrical gages to obtain movements with the soil mass.

Applications to Field Usage

The results of this study have several implications with respect to the practical application of field compactors. With all vibratory compactors, the most important output is the settlement produced by vibration. The results of this study indicate that in order to obtain the most settlement from a vibratory compactor the transmitted energy per load cycle must be maximized.

There are several system variations which may be utilized to maximize the transmitted energy per load cycle. This could be done by increasing the static weight of the compactor while holding all other variables constant. This is true since the transmitted energy is approximately equal to the product of the static weight and amplitude of vibration. This static weight increase could be accomplished in many ways; the most obvious would be to physically add weight to a vibrator. A second method which might be used to increase the effective static weight would be to sling the vibrating roller in a manner such that the yoke would offer resistance to the upward movement of the roller. This action would cause the average force acting on the sand to be larger than the static weight of the vibrator.

A second variation of the vibrator system which would increase the transmitted energy would be to maximize the amplitude of vibration. This can be done by increasing the dynamic force output of the vibrator. Since most field compactors generate the dynamic force using a rotating eccentric mass system, increasing the speed of rotation or size of excentric mass will increase the resulting amplitude of vibration. Because the dynamic force increases with the square of frequency of operation in an eccentric mass system, the largest amplitude of vibration may occur at frequencies above the resonant frequency.

CHAPTER XII

CONCLUSIONS

The following conclusions are based on the experimental results of laboratory tests using a five inch diameter vibrating circular plate acting on the surface of a dry sand.

1. The parameter which governs the ultimate settlement of a vibrating plate acting on dry sand is the steady-state transmitted energy per cycle of load application. This statement is valid for any initial relative density between 22 and 81 percent and for any frequency. Preliminary indications are that the concept of steady-state transmitted energy per cycle of load application may also be a useful technique for estimating the magnitude of settlement for times of vibration as short as 30 seconds.
2. Densification is a linear function of the logarithm of the steady-state transmitted energy per cycle of load application except for very low transmitted energy levels. These low transmitted energies are below the range of practical interest.

3. Ninety-five percent of the axial strain occurs within one diameter of the surface of the sand mass in most cases. This percentage is somewhat dependent on the transmitted energy of the vibrator; nevertheless, the surface movements below the centerline of the loaded area are attenuated very rapidly as distance below the surface increases.
4. Movements within the sand mass indicate that the zone of influence beneath the loaded area is not significantly affected by changing input variables (i.e. operation below, at and above the resonant frequency did not significantly change the zone of influence).

This study has several implications with respect to the practical use of field compactors.

1. Maximizing the transmitted energy will yield the best compaction.
2. Increasing the static weight, W, with all other variables being constant will increase the transmitted energy since transmitted energy is approximately equal to static weight times amplitude of vibration.
3. Increasing the dynamic force until the maximum amplitude of vibration is obtained, even if the

frequency is above resonance, will maximize transmitted energy. The maximum value for the dynamic force would be the static weight of the vibrator.

APPENDICES

APPENDIX A

SAND PROPERTIES

In order to characterize the sand, several tests were performed. These tests included moisture content, specific gravity, maximum density, minimum density, grain size distribution, and triaxial shear tests.

Two different sand samples were obtained from the sand mass. The sand was weighed, dried in an oven, and weighed a final time. The results as indicated by Table 12 for both tests were zero water content for the sand. This was to be expected since the sand was air dried every time the sand was rained into the test bin.

Table 12. Moisture Content Determination

Trial Number	1	2
Weight (Sand + Water + Tare)	398.51 gms	435.23 gms
Weight (Sand + Tare)	398.51 gms	435.23 gms
Weight (Water)	0.00 gms	0.00 gms
Moisture Content	0.0 %	0.0 %

Table 13 shows the data and results of three standard tests performed on sand samples to determine the

specific gravity of the sand. As Table 13 indicates, there was very little scatter in the results of the three tests.

Table 13. Specific Gravity Determination

Trial Number	1	2	3
Weight = W_{bws} (Flask + Sand + Water)	747.70 gms	746.20 gms	720.26 gms
Weight = W_{bw} (Flask + Water)	681.67 gms	681.20 gms	664.10 gms
Weight (Tare + Dry Sand)	395.77 gms	392.21 gms	412.00 gms
Weight (Tare)	289.90 gms	287.40 gms	321.65 gms
Weight = W_s (Dry Sand)	105.87 gms	104.81 gms	90.35 gms
$W_w = (W_s + W_{bw} - W_{bws})xa^*$	39.98 gms	39.95 gms	34.32 gms
$G = W_s/W_w$	2.647	2.623	2.632

$G_{avg} = 2.63$

*a = correction factor for temperature

Temperature = 28 degrees C

Therefore a = 1.0036 from Sowers (38)

The maximum and minimum densities were obtained after several different procedures and many tests were

performed. The maximum density was obtained by raining the sand into a container and then vibrating this container. The minimum density was obtained by a method which gave an almost infinite quantity of flow and approximately zero heights of fall for the sand. A two sectioned container was filled almost full with sand, and then the open end of the container was covered. The container was turned over as rapidly as possible and replaced on a level stand. The upper section of the container was carefully removed, and then the remaining section was weighed. This weight and the volume of the container gave the density of the sample. The results of all the tests to determine the maximum and minimum densities are given in Table 14.

Table 14. Maximum and Minimum Density Determination

Trial Number	Maximum Density (lbs/ft^3)	Minimum Density (lbs/ft^3)
1	104.66	87.21
2	104.96	87.57
3	105.09	86.93
4	105.17	86.98

Vacuum triaxial shear tests were performed on sand samples to determine the strength characteristics for this sand. These tests were performed on sand samples having relative densities ranging from 23 percent to 82 percent.

Table 15 indicates the results of these tests. The relationship between ϕ' angle and relative density of the sand is shown in Figure 31.

Table 15. Vacuum Triaxial Shear Results

Average D_R (Percent)	σ_3 (lbs/in^2)	σ_1 (lbs/in^2)	Average ϕ' (Degrees)
23.2	4.421 7.368 10.357	15.329 27.058 36.722	34.25
55.5	7.398 10.378	33.491 46.543	39.50
69.5	4.420 7.368 10.315	24.214 36.369 53.544	42.00
82.4	4.421 10.357	27.895 61.620	45.50

Using the ϕ' angles determined from the triaxial shear tests and corresponding relative densities, the bearing capacities for the five inch diameter test plate were calculated using Equation 8. These calculated bearing capacities were compared with the results of the static load tests. Table 16 gives this comparison of bearing capacities.

$$q = \left(\frac{\gamma B}{2}\right) \cdot (N_\gamma) \cdot (S) \qquad (8)$$

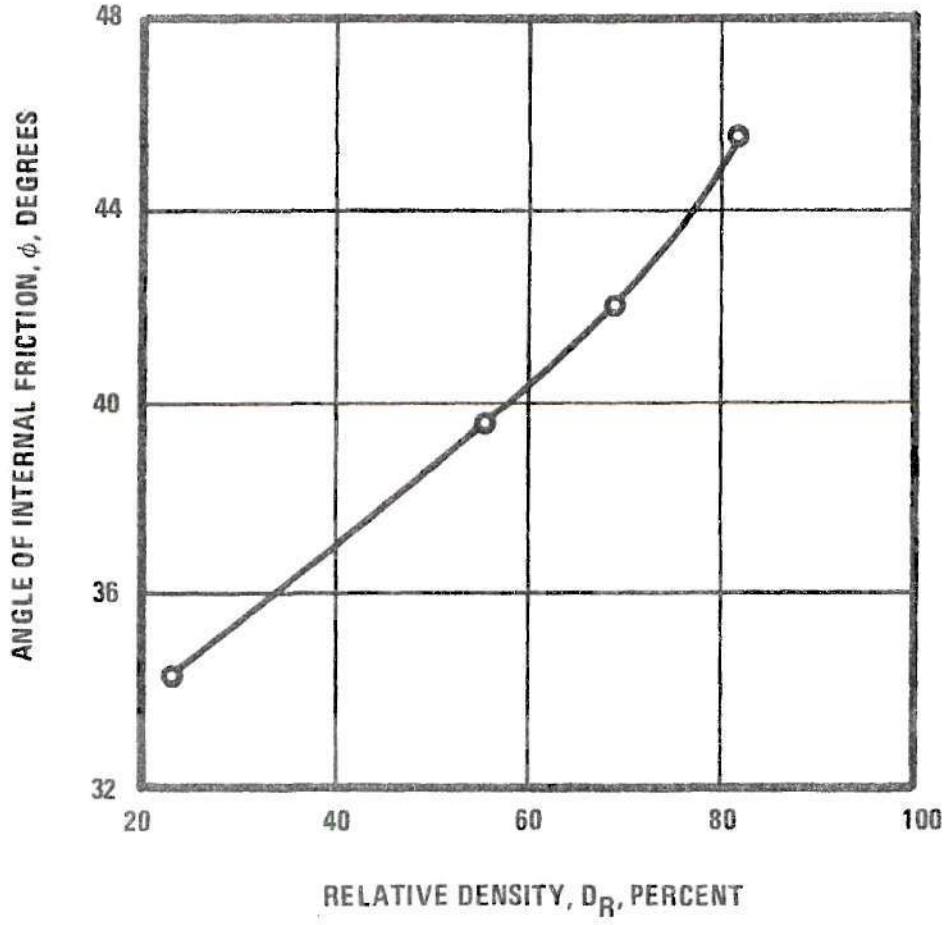

Figure 31. Angle of Internal Friction vs Relative Density

Where:

q = bearing capacity in pounds per square foot

γ = unit weight of sand in pounds per cubic foot

B = diameter of loading plate in feet

N_γ = Meyerhof's bearing-capacity factor

S = correction factor for circular footing

Table 16. Bearing Capacities

D_R (Percent)	Bearing Capacity (Pounds On A Five Inch Diameter Plate)	
	Static Test	Calculated
22	200	65
55	450	185
71	650	275
82	700	502

APPENDIX B

SOIL STRAIN GAGES

The Model 4101A soil strain gages used in this study were inductance coil type disks produced by Bison Instruments Inc. Two different size gages were used with their sizes being 1.125 inches in diameter by 0.125 inches thick and 2.125 inches in diameter by 0.250 inches thick. The gages were machined lined phenolic bases with electrical coils potted in epoxy for environmental stability. The gages were excited by a 20 KHz. frequency signal with a peak-to-peak amplitude of 15 volts. The maximum sensitivity of these gages was 0.0004 inches of movement per amplitude dial division.

The gages could be used with separations of the gages of from one to four diameters. The read-out unit had a control on it called the coil separation selector. The coil separation selector controlled the range over which the amplitude dial was effective. For gage separations of one to two diameters, two to three diameters, and three to four diameters, the coil separation selector was set at one, two or three. As this statement indicates, there was some overlap between the three ranges. Thus, by changing the coil separation selector, the sensitivity of the

read-out unit remained approximately constant for any gage separation.

The bridge balance in the read-out unit was accomplished by means of phase and amplitude controls using a meter to indicate null. After a null condition of both phase and amplitude was obtained for a given gage separation, the amplitude dial reading (0-1000 divisions) of the read-out unit corresponded to the sensor spacing. Changes in spacing were determined by renulling and noting the changes in the amplitude dial reading.

To establish the relationship between gage separation and null amplitude and phase dial reading for each coil separation range, each pair of gages was calibrated. The gages were placed on a device which could measure the distance between the gages to 0.001 inch. For each coil separation range, gage separations corresponding to null amplitude and phase dial readings at each 100 division from zero to 1000 were recorded. The relationship between gage separation and amplitude dial reading for a coil separation range of three is indicated in Figure 32 for a one inch set of gages, two inch set of gages, and a one inch-two inch set of gages. Similar relationships for coil separation ranges of one and two were obtained, but these ranges were rarely used and therefore are not indicated.

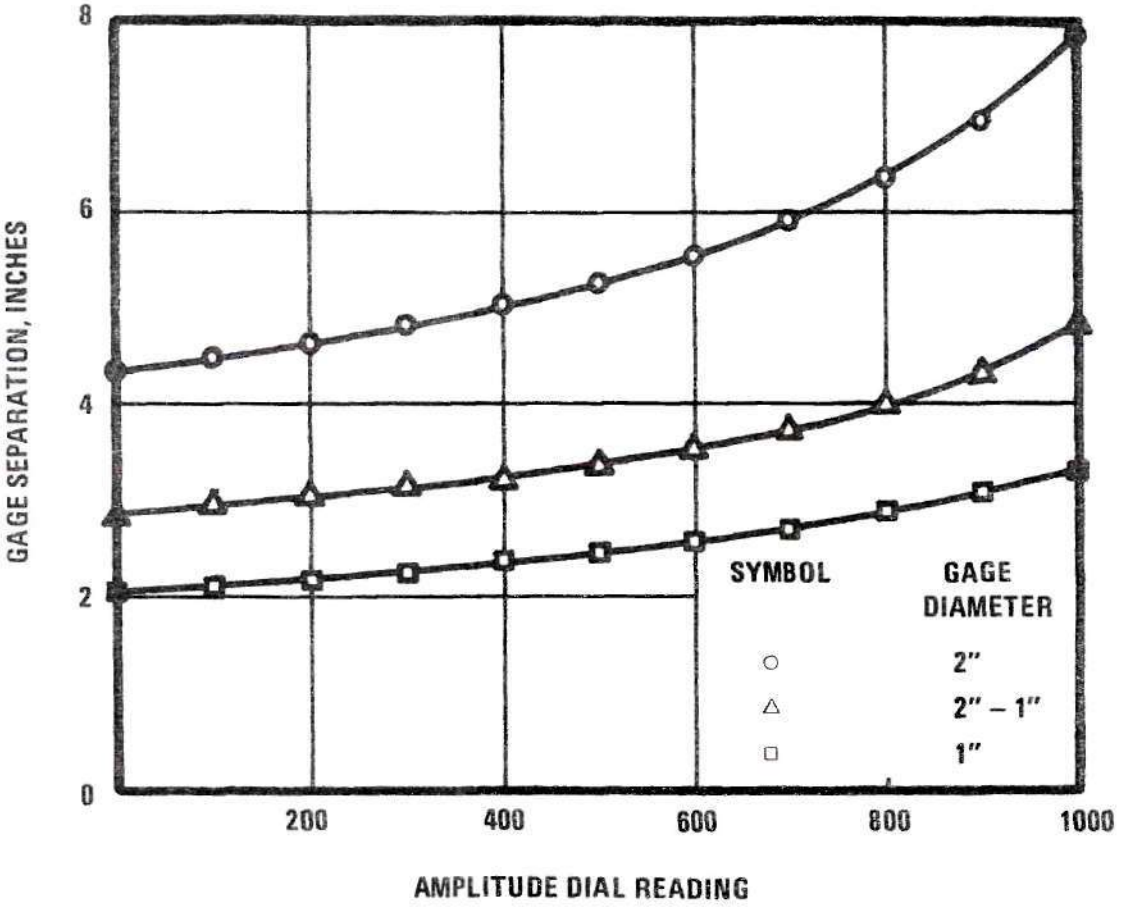

Figure 32. Amplitude Dial Reading vs Soil Strain Gage Separation

Two major problems were noted with these gages. First, the lead wires of the gages had to be shielded in order to obtain consistent results. Secondly, any metal within four diameters of any gage affected the output of the gage. Therefore, all metal, including the five inch diameter loading plate, was kept at least five diameters away from the nearest gage while any readings were being made.

APPENDIX C

SAND PLACEMENT APPARATUS

To insure that the actual relative density of the sand rained into the concrete block test bin corresponded to that calculated by dividing the weight of the sand rained into the bin by the volume of the bin, density samples were obtained from the sand mass. The density samples were obtained by forcing a piece of thin seamless circular tubing into the sand mass and excavating the sand from the interior of the tubing. By weighing the amount of sand excavated and dividing this weight by the volume of the excavation, the density of the sand was determined. This procedure was performed several times on freshly rained sand masses to obtain the relationship between the total sand mass density and the small sample sand density. Table 17 indicates that there was very little difference found between the two densities. Therefore, the density of the sand mass was taken to be that calculated by dividing the volume of the test bin into the total weight of sand rained into the test bin.

In order to establish the approximate relationship between hole alignment of the two bottom plates of the sand placement and relative density, the test bin was filled with

Table 17. Sand Mass Densities and Small Sand Sample Densities

Trial No.	Small Sample Density lbs/ft^3	Sand Mass Density lbs/ft^3
1	91.9	92.3
2	90.0	91.7
3	92.9	92.4
4	98.1	98.8
5	101.6	100.6

sand using different hole alignments. The hole alignment was obtained using steel stops which the lever struck upon moving. The relative distance from the support of these stops to their ends was the variable used to relate to the relative density of the sand. This relative distance is shown in Figure 33. Figure 34 indicates the results of these tests.

The relationship shown in Figure 34 was determined using an approximately constant height of fall for the sand particles of 16 inches. It was found that heights of fall three to four inches larger than or smaller than 16 inches did not appreciatively affect the relative density. This is in agreement with the results of Vesic (45) determined for the relationship between height of fall and density for a river sand.

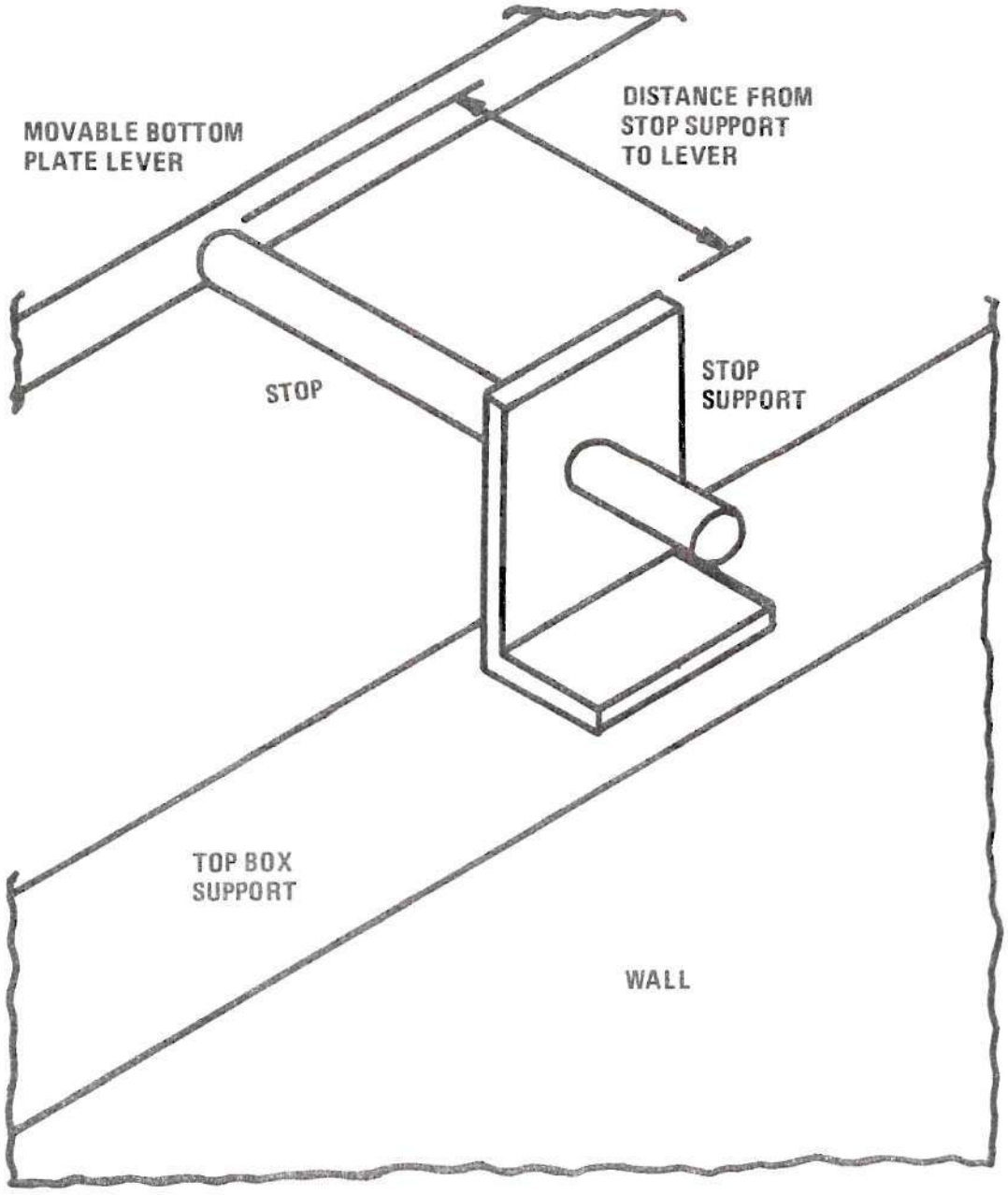

Figure 33. Sketch of Stop Support Mechanism of Sand Placement Box

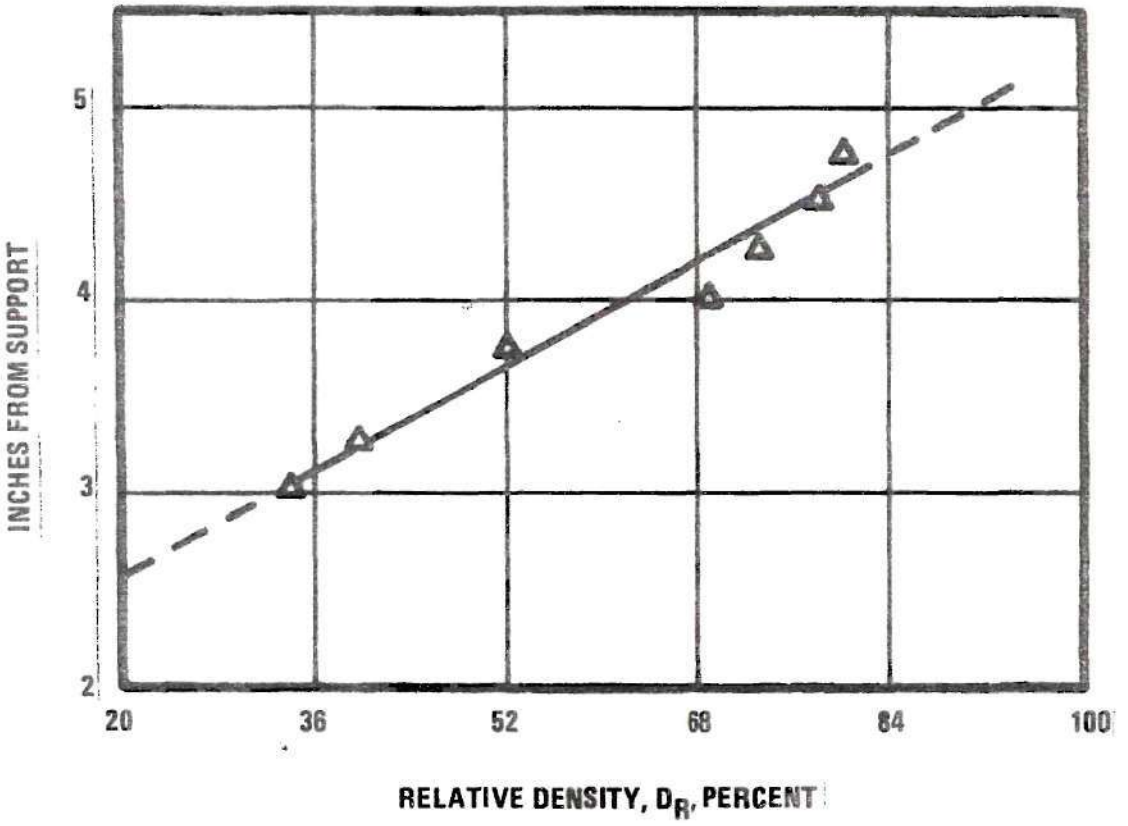

Figure 34. Relative Density vs Distance from Stop Support

APPENDIX D

SAMPLE CALCULATIONS

General

Sample calculations will be shown for test number 114, unconfined sample. The unit weight of the sand mass, relative density of the sand mass, final settlement of loading plate, amplitude of vibration of loading plate, transmitted energy, and soil strain gage movements will be calculated for this test. From Table 4 of Chapter X, the frequency of load application was 30 Hz., the static load was 100 pounds, and the dynamic loading was $\pm$80 pounds.

Calculations

From Table 4 of Chapter X , the weight of sand "rained" into the test bin was 5871.8 pounds. The volume of the lined test bin was 59.46 cubic feet. The unit weight of the sand mass was calculated using Equation 9.

$$\text{Unit Weight} = \gamma = \frac{\text{Weight}}{\text{Volume}} \qquad (9)$$

$$\gamma = \frac{5871.8 \text{ lbs}}{59.46 \text{ ft}^3}$$

$$\gamma = 98.75 \text{ lbs/ft}^3$$

Using "the" maximum and minimum unit weights for this sand from Table 14 of Appendix A and the unit weight of the sand for this test, the relative density of the sand was calculated using Equation 10 below.

$$D_R = (A) \times (B) \times 100\% \tag{10}$$

$$D_R = 69.02\%$$

$$A = \frac{\gamma - \gamma \text{ min}}{\gamma \text{ max} - \gamma \text{ min}} \tag{11}$$

$$A = \frac{98.75 \text{ lbs/ft}^3 - 86.93 \text{ lbs/ft}^3}{105.17 \text{ lbs/ft}^3 - 86.93 \text{ lbs/ft}^3}$$

$$B = \frac{\gamma \text{ max}}{\gamma} \tag{12}$$

$$B = \frac{105.17 \text{ lbs/ft}^3}{98.75 \text{ lbs/ft}^3}$$

The final settlement of the plate was determined by converting the D.C. voltage output of the LVDT as registered on the Mark 280 brush recorder into inches. Full range output for the LVDT was 10 volts, and this corresponded to a movement of 1.25 inches. Therefore, the conversion factor for changing volts of output into inches of movement was 0.125 inches/volt. For test 114 the D.C. voltage output of the LVDT was 3.92 volts. Therefore, using the above conversion factor the final settlement for

this test was

$$S_{60} = \text{(D.C. voltage output) X (0.125 inches/volt)} \quad (13)$$

$$S_{60} = \text{(3.92 volts) X (0.125 inches/volt)}$$

$$S_{60} = 0.490 \text{ inches}$$

The amplitude of vibration was calculated by converting the peak to peak A.C. voltage output of the external LVDT into inches. The conversion factor for this LVDT was 0.0054 inches/volt. The peak to peak A.C. voltage output was measured at 0.548 volts. Therefore, the amplitude of vibration was

$$A_p = \text{(A.C. voltage output) X (0.0054 inches/volt)} \quad (14)$$

$$A_p = \text{(0.548 volts) X (0.0054 inches/volt)}$$

$$A_p = 0.00298 \text{ inches}$$

The transmitted energy was calculated from Equation 6 of Chapter IV.

$$E_{TR} = F_{TR}(\text{lbs}) \text{ X } A_p \text{ (inches)} \quad (6)$$

$$E_{TR} = \text{(100 lbs) X (0.00298 inches)}$$

$$E_{TR} = 0.298 \text{ in-lbs}$$

F_d = dynamic force

The conversion of the soil strain gage data into gage separation, depths of gage embedment, strains, and normalized movement required several steps. The separation or distance from the original surface of the sand to the top of gage one was physically measured and is indicated in Table 18. The separation distances between gages one and two, two and three, three and four, four and five, and five and six were determined by converting the null amplitude dial output of the soil strain gage unit into inches using Figure 32 of Appendix B. This conversion gave the initial (before dynamic loading) and final (after dynamic loading) gage separations indicated in Table 18.

Table 18. Soil Strain Gage Separations

Gage Numbers	Initial Separations (Inches)	Final Separations (Inches)
Surface to 1	0.787	1.120
1 to 2	3.081	2.885
2 to 3	2.964	2.915
3 to 4	3.136	3.106
4 to 5	4.784	4.773
5 to 6	5.821	5.821

Depths from the original sand surface to the tops of the gages were determined in the manner described in

this section. The depth to the top of the second gage was determined by adding to the depth of the first gage the thickness of that gage and then adding the electronically measured distance between gage one and two.

The depth to the third gage was obtained by adding the thickness of the second gage and the electronically measured distance between the second and third gage to the depth to the top of the second gage.

This cumulative process was continued until the depth below the surface of the lowest gage was determined. These same steps were followed to find the embedment depths both before and after a sample had been dynamically loaded. The following calculations present the initial gage depths for this test.

$$\text{Depth} = A + B + C \tag{15}$$

A = depth to top of gage above

B = thickness of gage above

C = gage separation distance

For Gage 1 (0.125 inches thick):

Initial Depth = 0 inches + 0 inches + 0.787 inches

Initial Depth = 0.787 inches

For Gage 2 (0.125 inches thick):

Initial Depth = 0.787 inches + 0.125 inches + 3.081 inches

Initial Depth = 3.993 inches

For Gage 3 (0.125 inches thick):

Initial Depth = 3.993 inches + 0.125 inches + 2.964 inches

Initial Depth = 7.082 inches

For Gage 4 (0.125 inches thick):

Initial Depth = 7.082 inches + 0.125 inches + 3.136 inches

Initial Depth = 10.343 inches

For Gage 5 (0.250 inches thick):

Initial Depth = 10.343 inches + 0.125 inches + 4.784 inches

Initial Depth = 15.252 inches

For Gage 6 (0.250 inches thick):

Initial Depth = 15.252 inches + 0.250 inches + 5.821 inches

Initial Depth = 21.323 inches

This same procedure was followed to determine the depths of embedment after the dynamic loading. Table 19 indicates the depths of embedment of the gages.

Table 19. Depths of Gage Embedment

Gage Numbers	Initial Depth of Embedment (Inches)	Final Depth of Embedment (Inches)
1	0.787	1.120
2	3.993	4.130
3	7.082	7.170
4	10.343	10.401
5	15.252	15.292
6	21.323	21.370

The values of strain which were plotted in Figure 24 of Chapter IX were obtained by using Equation 16 below.

$$\text{Strain} = \frac{L' - L}{L} \times 100\% \qquad (16)$$

L = original gage separation distance

L' = final gage separation distance

For Gages 1 and 2: from Table 6

$$\text{Strain} = \frac{4.130 - 3.993}{3.993} \times 100\% = 4.5\%$$

$L = 3.993$ inches

$L' = 4.130$ inches

The values of normalized movement which were used in Figure 26 of Chapter X were calculated using Equation 17.

$$N.M. = \frac{F.D. - I.D.}{S_{60}} \times 100\% \qquad (17)$$

N.M. = Normalized Movement

I.D. = Initial Depth of Gage

F.D. = Final Depth of Gage

S_{60} = Five Inch Diameter Plate Settlement at 60 Minutes

For Gage 2: from Table 6

I.D. = 3.993 inches

F.D. = 4.130 inches

$$N.M. = \frac{4.130 \text{ in} - 3.993 \text{ in}}{3.993 \text{ in}} \times 100\%$$

N.M. = 3.43%

BIBLIOGRAPHY

BIBLIOGRAPHY

1. Barkan, D. D., Dynamics of Bases and Foundations, translated from Russian by Drashevska, L., McGraw-Hill Book Company, New York, 1962.

2. Barkan, D. D., "Developments in Soil Dynamics," Proceedings International Symposium on Wave Propagation and Dynamic Properties of Earth Materials, University of New Mexico, August 1967.

3. Broms, B. B. and Forssblad, L., "Vibratory Compaction of Cohesionless Soils," Soil Dynamics Specialty Conference, Seventh International Conference on Soil Mechanics and Foundation Engineering, Mexico City, August 1969.

4. Brumund, W. F., "Subsidence of Sand Due to Surface Vibration," Ph.D. Thesis, Purdue University, Lafayette, Indiana, 1969.

5. Brumund, W. F. and Leonards, G. A., "Subsidence of Sand Due to Surface Vibration," Journal of Soil Mechanics and Foundations Division, ASCE, Vol. 98, No. SM 1, January 1972.

6. Chae, Yong S., "Dynamic Behavior of Embedded Foundation-Soil System," presented at Highway Research Board 49th Annual Meeting, January, 1970.

7. Converse, F. J., "Compaction of Sand at Resonant Frequency,", ASTM Special Technical Publication No. 156, "Symposium on Dynamic Testing of Soils," 1953, pp. 124-137.

8. D'Appolonia, D. J. and D'Appolonia, E., "Determination of the Maximum Density of Cohesionless Soils," Proceedings The Third Asian Regional Conference on Soil Mechanics and Foundation Engineering, International Society of Soil Mechanics and Foundation Engineering, Israel, 1967, Vol. 1.

9. D'Appolonia, D. J., Whitman, R. V., and D'Appolonia, E., "Sand Compaction with Vibratory Rollers," Journal of the Soil Mechanics and Foundations Division, ASCE, Vol. 95, No. SM 1, January 1969.

10. D'Appolonia, E., "Dynamic Loadings," ASCE Specialty Conference on Placement and Improvement of Soil to Support Structures, Massachusetts Institute of Technology, 1968.

11. D'Appolonia, E., "Densification of Granular Soils by Vibration," The University of Michigan Engineering Summer Conferences Vibrations of Soils and Foundations, June 1968.

12. Eastwood, W., "Vibrations in Foundations," The Structural Engineer, The Journal of the Institution of Structural Engineers, England, March 1953, Vol. 31, pp. 82-98.

13. Forssblad, L., "Investigation of Soil Compaction by Vibration," Acta Polytechnica Scandinavica, Civil Engineering and Building Construction Series No. 34, 1965.

14. Fry, Z. B., "Development and Evaluation of Soil Bearing Capacity Foundations of Structures - Field Vibratory Tests Data, " U.S. Army Engineer Waterways Experiment Station, Vicksburg, Mississippi, Technical Report No. 3-632, July 1963.

15. Greenfield, B. J. and Misiaszek, E. T., "Vibration-Settlement Characteristics of Four Gradations of Ottawa Sand, " Proceedings, International Symposium on Wave Propagation of Earth Materials, University of New Mexico, August 1967.

16. Hertwig, A., Fruh, G. and Lorenz, H., "Determination of Soil Characteristics with Reference to Structures by Means of Forced Vibrations," (in German), German Society of Soil Mechanics (Degebo), 1933, No. 1.

17. Ho, M. M. K., and Burwash, W. J., "Vertical Vibration of a Rigid Foundation Resting on Sand," A Paper Presented at the 71st Annual Meeting of the American Society of Testing and Materials, June 1968.

18. Johnson, A. W. and Sallbert, J. R., "Factors that Influence Field Compaction of Soils," Highway Research Board Bulletin 272, 1960.

19. Kolbuszewski, J. J., "An Experimental Study of the Maximum and Minimum Porosities of Sands, " Proceedings Second International Conference on Soil Mechanics and Foundation Engineering, Rotterdam, 1948, Vol. 1, pp. 158-165.

20. Krumbein, W. C. and Sloss, L. L., Stratigraphy and Sedimentation, W. H. Freeman and Company, San Francisco, 1963.

21. Lewis, W. A., "Full-Scale Compaction Studies at the British Road Research Laboratory," Highway Research Board Bulletin 254, "Soil Compaction and Proof-Rolling of Subgrades," 1960, pp. 1-11.

22. Lewis, W. A., "Recent Research into the Compaction of Soil by Vibratory Compaction Equipment," Proceedings Fifth International Conference on Soil Mechanics and Foundation Engineering, Paris, 1061, Vol. II, pp. 261-268.

23. Lysmer, J., "Vertical Motion of Rigid Footings," Ph.D. Dissertation, University of Michigan, Ann Arbor, August 1965.

24. Lysmer, J. and Richart, F. E., "Dynamic Response of Footings to Vertical Loading, " Journal of Soil Mechanics and Foundation Division, ASCE, Vol. 92, No. SM 1, January 1966.

25. Mogami, T. and Kubo, K., "The Behavior of Soil During Vibration," Proceedings of the Third International Conference on Soil Mechanics and Foundation Engineering, Switzerland, 1953, Volume I, pp. 152-155.

26. Moore, P. J., "Calculated and Observed Vibrational Amplitudes", Journal of Soil Mechanics and Foundation Division, ASCE, Vol. 97, No. SM 1, January 1971.

27. Moorhouse, D. C. and Baker, G. L., "Sand Densification by a Heavy Vibratory Compactor," ASCE Specialty Conference on Placement and Improvement of Soil to Support Structures, Massachusetts Institute of Technology, 1968.

28. Novak, M., "Prediction of Footing Vibrations," Journal of Soil Mechanics and Foundation Division, ASCE, Vol. 96, No. SM 3, May 1970.

29. Orgigosa, P., "Densification of Sand by Vertical Vibrations with Almost Constant Stresses," Massachusetts Institute of Technology, Department of Civil Engineering, Soils Publication No. 206, January 1968.

30. Prakash, S., and Gupta, M. K., "Compaction of Sand Under Vertical and Horizontal Vibrations," South East Asian Conference on Soil Mechanics and Foundation Engineering, Bangkok, 1967.

31. Quinlan, P. M., "The Elastic Theory of Soil Dynamics," ASTM Special Technical Publication No. 156, "Symposium on Dynamic Testing of Soils," 1953, pp. 3-34.

32. Reissner, E., "Stationare, axialsymmetrische durch eine schuttelnde Masse erregte Schwingungen eines homogenen elastischen Halbraumes," Ingenieur-Archiv, Vol. 7, No. 6, December 1936, pp. 381-396.

33. Richart, F. E., "Foundation Vibrations," Journal of the Soil Mechanics and Foundations Division, ASCE, Vol. 86, No. SM 4, August 1960.

34. Richart, F. E. and Whitman, R. V., "Comparison of Footing Vibration Tests with Theory," Journal of the Soil Mechanics and Foundations Division, ASCE, Vol. 93, No. SM 6, November 1967.

35. Robson, J. D., "Effects of Non-Linearity on the Resonant Frequency of a Body of Soil," 9th International Congress of Applied Mechanics, Brussels, 1956, Vol. 7, pp. 344-349.

36. Selig, E. T., " Applications of Strain Measurements to Soil Compaction Evaluation," Paper Presented at 52nd Annual Meeting Highway Research Board, Washington, D. C., January 1973.

37. Silver, M. L. and Seed, H. B., "Volume Changes in Sands During Cyclic Loading," Journal Soil Mechanics and Foundations Division, ASCE, Vol. 97, No. SM 9, September 1971.

38. Sowers, G. F., and Scholtes, R. M., Laboratory Manual for Soil Testing, Georgia Institute of Technology, Atlanta, Georgia, 1962.

39. Sung, T. Y., "Vibrations in Semi-Infinite Solids Due to Periodic Surface Loadings," ASTM Special Technical Publication No. 156, "Symposium on Dynamic Testing of Soils," 1953, pp. 35-63.

40. Tanimoto, K., "On the Compaction of Soil by Surface Vibration Load," Memoirs of the Faculty of Engineering Kobe University, 1960, Japan.

41. Taylor, C., Green, R., and Kalita, U. C., "Factors Affecting the Response of Machine Foundations," Proceedings International Symposium on Wave Propagation of Earth Materials, University of New Mexico, August 1967.

42. Timmerman, D. H. and Wu, T. H., "Behavior of Dry Sands Under Cyclic Loading," Journal of Soil Mechanics and Foundations Division, ASCE, Vol. 95, No. SM 4, July, 1969.

43. Thomson, W. T., Mechanical Vibrations, 2nd Edition, Prentice-Hall Inc., Englewood Cliffs, N. J., 1962.

44. Tschebotarioff, G. P. and McAlpin, G. W., "The Effect of Vibratory and Slow Repetitional Forces on the Bearing Properties of Soils," Civil Aeronautics Administration Technical Development Report No. 57, U.S. Department of Commerce, October 1947.

45. Vesic, A. S., "A Study of Bearing Capacity of Deep Foundations," Engineering Experiment Station, Georgia Institute of Technology, Project B-189 Final Report, 1967.

46. Walker, B. P. and Whitaker, T., "An Apparatus for Forming Uniform Beds of Sand for Model Foundation Tests," Geotechnique, Vol. 17, No. 2, June 1967, pp. 161-167.

47. Whitman, R. V., and Origosa, P., "Densification of Sand by Vertical Vibration," Massachusetts Institute of Technology, Department of Civil Engineering, Soils Publication No. 222, August 1968.

48. Whitman, R. V. and Richart, F. E., "Design Procedures for Dynamically Loaded Foundations," Journal of the Soil Mechanics and Foundation Division, ASCE, Vol. 92, No. SM 6, November 1967.

49. Youd, T. L., "Compaction of Sands by Repeated Shear Straining," Journal of Soil Mechanics and Foundation Division, ASCE, Vol. 98, No. SM 7, July 1972.

VITA

Joe F. Skelton was born in Amarillo, Texas, on July 8, 1945, the son of Juanita K. Skelton and Hiram Bowmer Skelton. After graduating in 1963 from Arlington High School, Arlington, Texas, he entered The University of Texas at Arlington. He received the degree of Bachelor of Science in Civil Engineering in 1968 and the degree of Master of Science in Civil Engineering in 1969 from The University of Texas at Arlington. In September, 1969, he entered the Graduate School of Georgia Institute of Technology in Atlanta, Georgia.

He is married to the former Deanna Evans, and they have one daughter, Lucinda Dee.